Characterization of painting pigments and ochres associated with the Hoabinhian archaeological context at the rock-shelter site of Doi Pha Kan (Thailand)

Matthieu Lebon, Xavier Gallet, Manon Bondetti, Sylvain Pont, Guilhem Mauran, Philippe Walter, Ludovic Bellot-Gurlet, Simon Puaud, Antoine Zazzo, Hubert Forestier, et al.

Characterization of painting pigments and ochres associated to the Hoabinhian archaeological context at the rock-shelter site of Doi Pha Kan (Thailand)

Lebon M.[1], Gallet X.[1], Bondetti M.[2,3], Pont S.[4], Mauran G.[1], Walter P.[5], Bellot-Gurlet L.[6], Puaud S.[1], Zazzo A.[4], Forestier H.[8], Auetrakulvit P.[9], Zeitoun V.[10]

1 - UMR7194 - Histoire Naturelle de l'Homme Préhistorique (HNHP), Muséum national d'Histoire naturelle, CNRS, Université Perpignan Via Domitia, Musée de l'Homme, 17, Place du Trocadéro 75116 Paris - France

2 - BioArch, University of York, Heslington, YO10 5DD, United Kingdom

3 - Arctic Centre, University of Groningen, Aweg 30, 9718CW Groningen, The Netherland

4 - UMR 7590 - Institut de Minéralogie, de Physique des Matériaux et de Cosmochimie (IMPMC), Muséum national d'Histoire naturelle, CNRS, Sorbonne Université, IRD. 61 rue Buffon, 75005 Paris, France.

5 – UMR 8220 – Laboratoire d'Archéologie Moléculaire et Structurale (LAMS), Sorbonne Université, CNRS, 4 place Jussieu, 75005, Paris, France

6 – UMR 8233 - De la molécule aux nano-objets: réactivité, interactions et spectroscopies (MONARIS), Sorbonne Université, CNRS, , 4 place Jussieu, 75005, Paris, France

7. UMR 7209 - Archéozoologie, Archéobotanique: Sociétés, pratiques et environnements (AASPE), Muséum national d'Histoire naturelle, CNRS, CP 56, 55 rue Buffon, 75005 Paris, France

8. UMR7194 - Histoire Naturelle de l'Homme Préhistorique (HNHP), Muséum national d'Histoire naturelle, CNRS, Université Perpignan Via Domitia, Musée de l'Homme, 17, Place 1 rue René Panhard, 75013 Paris, France

9. Department of Archaeology, Faculty of Archaeology, Silpakorn University, Na Phra road, 10220 Bangkok, Thailand

10 UMR 7207 - Centre de Recherche en Paléontologie- Paris (CR2P), CNRS, Sorbonne Université, Muséum national d'Histoire naturelle, 4, place Jussieu, 75005 Paris, France

Abstract :

The use of ochre in mortuary practices was widespread during prehistory. In northern Thailand, several painted rock-shelters attributed to Iron age or Neolithic cultures have provided burials characterized by the presence of pigment fragments and ochres deposits. In the case of Doi Pha Kan, data collected during excavations have highlighted the important role of ochre in funerary rites dating from 11,170 ± 40 to 12,930 ± 50 BP. The presence of painted panels overhanging Hoabinhian burials raises the question of their chronology and association to painting activities. To investigate this issue at Doi Pha Kan, we applied a multi-analytical approach (optical microscopy, SEM-EDS, Raman spectroscopy, XRF spectroscopy) on painting pigments and ochres associated to a grave (dpk E-5) and the archaeological context to determine the mineralogical and elemental composition of pigment raw materials. We showed that the composition of raw pigments from the archaeological context is homogeneous, suggesting a common geological source characterized by the presence of As. In contrast, pigments on the painted panel have variable compositions indicating that panels were created in different time periods. The pigment used for anthropomorphic figure is the only one similar to the materials identified in the archaeological levels and burial at Doi Pha Kan. Without possibility of direct dating, it is not possible to establish a direct link between the these anthropomorphic figure paintings and mortuary practices, however two painted wall fragments were discovered in the archaeological layers attest to a long tradition of rock painting for at least 11,000 years at this site.

1/ Introduction

The use of ochre or red pigment in mortuary practices has been globally widespread since the Paleolithic, and can be observed in the famous sites of Qafzeh in the Near East (Bar-Yosef Mayer, et al., 2009), Dolní Věstonice in the Czech Republic (Klima, 1987), Lake Mungo 3 in Australia (Thorne, et al., 1999) and Cro-Magnon in France (Henry-Gambier, 2002). In Southeast Asia, ochre has been commonly reported in burial contexts from the late Bronze Age and Iron Age periods in northeastern Thailand (O'Reilly, 2014, Higham, 2011), but it is rarely reported in the literature.

For the Hoabinhian period, spanning from 30,000 to 3000 BP in Southeast Asia (Imdirakphol, et al., 2017), references are rarer, but the use of ochre in graves was noted in northern Vietnam in the Con Moong cave around 11 – 12,000 BP (Thong, 1980, Ha, 1980), in southern Vietnam at the Con Co Ngua site belonging to the Da But Culture (6000 to 6500 BP) (Oxenham, 2006), in northern Malaysia at Gua Gunung Runtuh for graves dated between 9460 ± 90 and 10,120 ± 110 BP (Jacob and Soepriyo, 1994, Zuraina, 1994) and at Gua Teluk Kelawar for a grave dated between 8400 ± 40 and 10,245 ± 80 BP (Zuraina, 2005), and in central Thailand at Sai-Yok cave, dated between 4000 BP and 10,000 BP (Van Heekeren, 1961, Jacob, 1969).

In northern Thailand, three Hoabinhian sites in the Mae Moh district have provided several burials characterized by the presence of ochre deposits (Imdirakphol, et al., 2017). Phratu Pha site is the largest painted rock-shelter in northern Thailand, and five burials have been dated to about 3000 BP (Doy Asa, et al., 2001, Srongsiri and Sangchan, 1997). Recent excavations of Ban Than Si uncovered an individual burial dated to 7000 BP. At Doi Pha Kan, graves were uncovered and the radiocarbon ages obtained range from 11,170 ± 40 to 12,930 ± 50 BP, attributing them to the Hoabinhian culture (Imdirakphol, et al., 2017). Data collected during the excavations at Doi Pha Kan has highlighted the important role of ochre in funerary rites (Imdirakphol, et al., 2017).

Hundreds of painted caves and rock-shelter sites are known in Thailand, dating from prehistoric to modern periods (Tan and Taçon, 2014). Figurations often lack direct chronological contextualization, but they are mainly attributed to the Iron Age and associated with sedentary pastoral societies (Higham, 2002). However, recent work based on stylistic approaches and the superimposition of figures suggests an earlier age for some figurations in mainland Southeast Asia. Likewise, direct radiocarbon and U-series dating revealed Pleistocene ages for some sites in Borneo, East Timor and Sulawesi (Taçon, et al., 2014, Aubert, et al., 2014, Aubert, et al., 2007, Aubert, et al., 2018).

The presence of paintings on panels overhanging the Hoabinhian and Neolithic sites of the Phratu Pha Valley raises the question of their associations and the chronology of painting activities (Surinlert, et al., 2018). Even if it is difficult to make a direct chronological connection between paintings and human settlements or burials, studies involving several analytical approaches have been developed to determine the chronology of such archaeological contexts. These approaches include the identification of material likely to provide geochronological data, for example, calcite deposits or oxalate crusts that provide samples for 14C dating (Aubert, et al.,

2014, Jones, et al., 2017). A comparative study of the pigments present in archaeological levels and those covering painted walls, or fragments of painted walls, can also provide clues on the temporality of these material expressions (Beck, et al., 2011, Lebon, et al., 2014). Furthermore, studying the superimposition of pigments layers, position between them, and with alteration crusts/deposits of weathering minerals, can reconstruct the relative chronology of paintings (Chalmin, et al., 2017a, Chalmin, et al., 2017b).

Following methodologies developed in the studies cited above, we used a multi-analytical approach to analyse pigments and raw materials used at the Doi Pha Kan (DPK) rock shelter. The mineralogical and elemental composition of raw materials associated with a grave (dpk E-5) and in surrounding sediment was compared with the composition of pigments deposited on archaeological artifacts. Particular focus was given to characterise the samples collected from the painted wall. The results were compared with archaeological materials in order test the possible link between between the burial activities and rock paintings at this Hoabinhian site

2/ Material and method

2.1 Archaeological context of Doi Pha Kan

Doi Pha Kan (N 18° 26.95' E 99° 46.62') is a painted rock-shelter 20 meters in length located in the district of Mae Moh, 3 km north of Ban Tha Si, 7 km south of the rock art painting site of Phratu Pha. The rock-shelter site opens up in the eastern wall of the limestone Doi Pha Kan mountain. Several painted figures are present on the wall, between 1.5 and 3.5 m above ground level (area C2/D2 – Fig. 1a). The wall has been significantly altered by water runoff, but some parts are better preserved due to protection by rock overhangs (Fig. 1b). Several figures of animals (carnivores, proboscideans, bovids and a gallinacaea) associated to hand and anthropomorphic forms, as well as geometric figures, have been identified (Surinlert, et al., 2018).

Doi Pha Kan deposits are powdery loamy sediments accumulated over a depth of at least two meters (Imdirakphol, et al., 2017, Zeitoun, et al., 2019). Due to the loose nature of the sediment, large excavations were not possible without disturbing sediments and the embedded archaeological remains. Therefore, the site was excavated by opening up small successive trenches less than 90 cm deep. The archaeological context is marked by the presence of burials that have disturbed the sediment (three burials have been excavated to date). The mean density of the material was high with 3109 artifacts per m^3, but no distinctive layers could be identified during the excavation. Due to this particular stratigraphical context, it was difficult to date the archaeological material nearby the graves. However, radiocarbon direct dating of anthropological remains provided dates ranging from 11,170 ± 40 to 12,930 ± 50 BP for the three graves (Zeitoun, et al., 2019). These dates obtained on bioapatite are consistent with those obtained for charcoal (12,930 ± 40 BP) and shell (12,920 ± 80 BP). The graves dpk D-4 (12,719-12,081 BC Cal) and dpk E-5 (13,169-12,462 BC Cal) are deeper (Z = 90-120 cm) than the grave dpk DE-5 (11,955-11,641 CB cal) that is more superficial (Z = 40-60) and was found 30 cm above the grave dpk D-4. The dating of these burials provides a minimum age for the surrounding sediment and associated archaeological material, which are logically older than the burials themselves.

In the grave dpk E-5, the skeleton was covered and surrounded by ochre powder. This grave is also characterized by the presence of ochre fragments and a faceted ochre block (Fig. 2: E5-B1

and E5-317), and some gifts: a reddish subtriangular-shaped perforated stone whose form suggests a pendant (Fig. 2: E5-286), a perforated stone and two grinding tools colored by ochre (e.g. Fig. 2: D6-383).

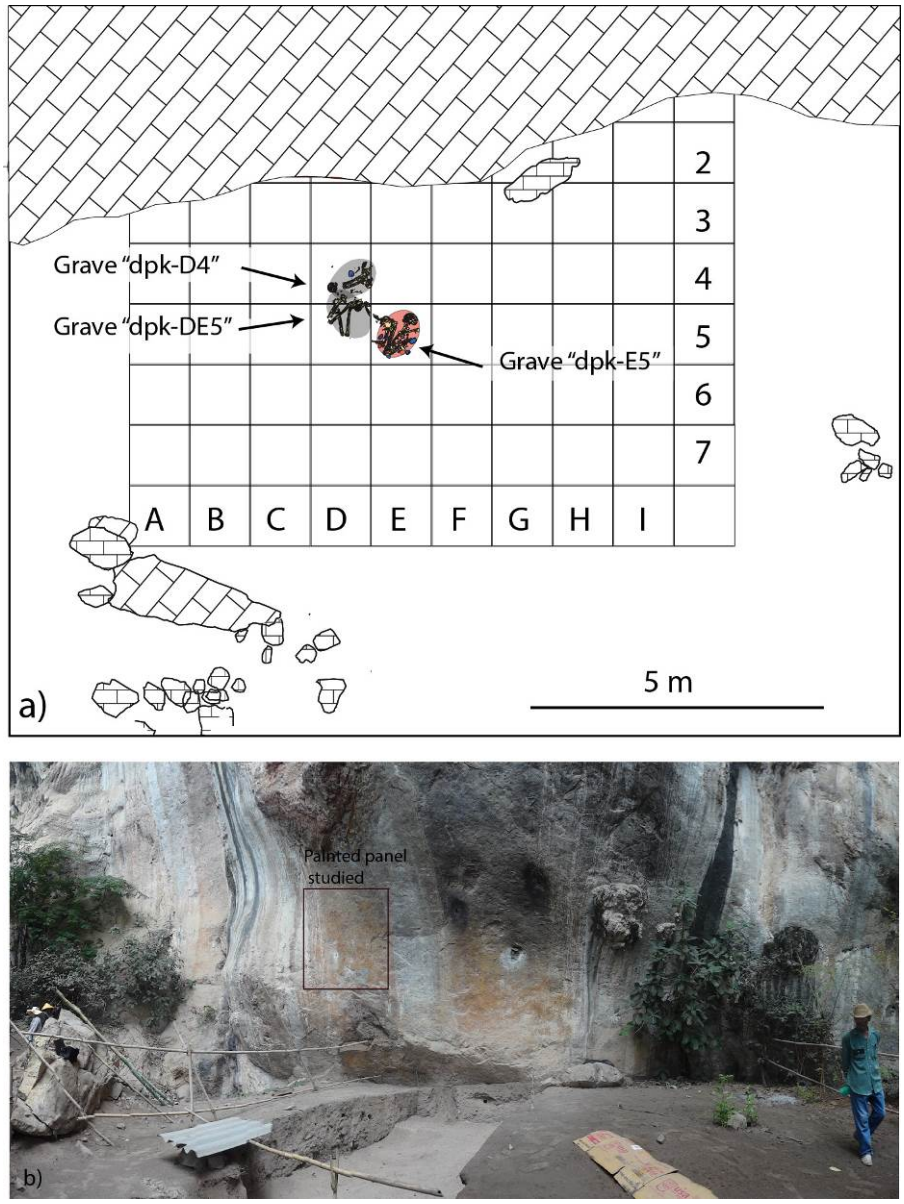

Fig. 1. a) Location of the excavated area, graves and painted panel at Doi Pha Kan. b) Photograph of the excavated area and location of the painted panel .

2.2 Material

Archaeological samples from the grave dpk-E5 and archaeological levels excavated at DPK include a faceted block (n=1), block fragments (n=7), and powders (n=2) identified as ochre or raw pigments - red rocks rich in iron oxides (hematite). Several artifacts were also studied: a grinding stone (D6-323), a fragment of pebble with residues of pigment powder (I3-103), a flat pebble covered by a cohesive deposit of pigment and interpreted as a painted pebble (D7-413), a perforated stone (G6-119), a colored subtriangular-shaped perforated stone suggesting a pendant (E5-286), and a handstone/grinder (E5-15). The origin and nature of the samples are detailed in Table 1 and Fig. 2 shows photographs of a representative selection of this material..

To investigate the composition of pigments used for the paintings at the DPK site, several samples were collected from the painted panel presented in Fig. 3 . To limit the invasiveness of this sampling procedure, small fragments already partially detached from the limestone wall where selected and carefully removed using a scalpel blade (Fig. 3d-e). These sample fragments were photographed, observed under a Hirox microscope and then polished cross sections were prepared to access the stratigraphy of deposits over bedrock. Six samples were collected from the DPK painted wall including five pigmented samples from different stylistic groups of figures (established by Surinlert, (2013) and one non-pigmented sample to access the alteration state of the bedrock.

Fig. 2. Photographs of a selection of raw pigments and artifacts displaying red hues or pigment deposits from graves or archaeological layers at Doi Pha Kan (DPK) site and analyzed in this study. For each image, the scale bar correspond to 1 cm.

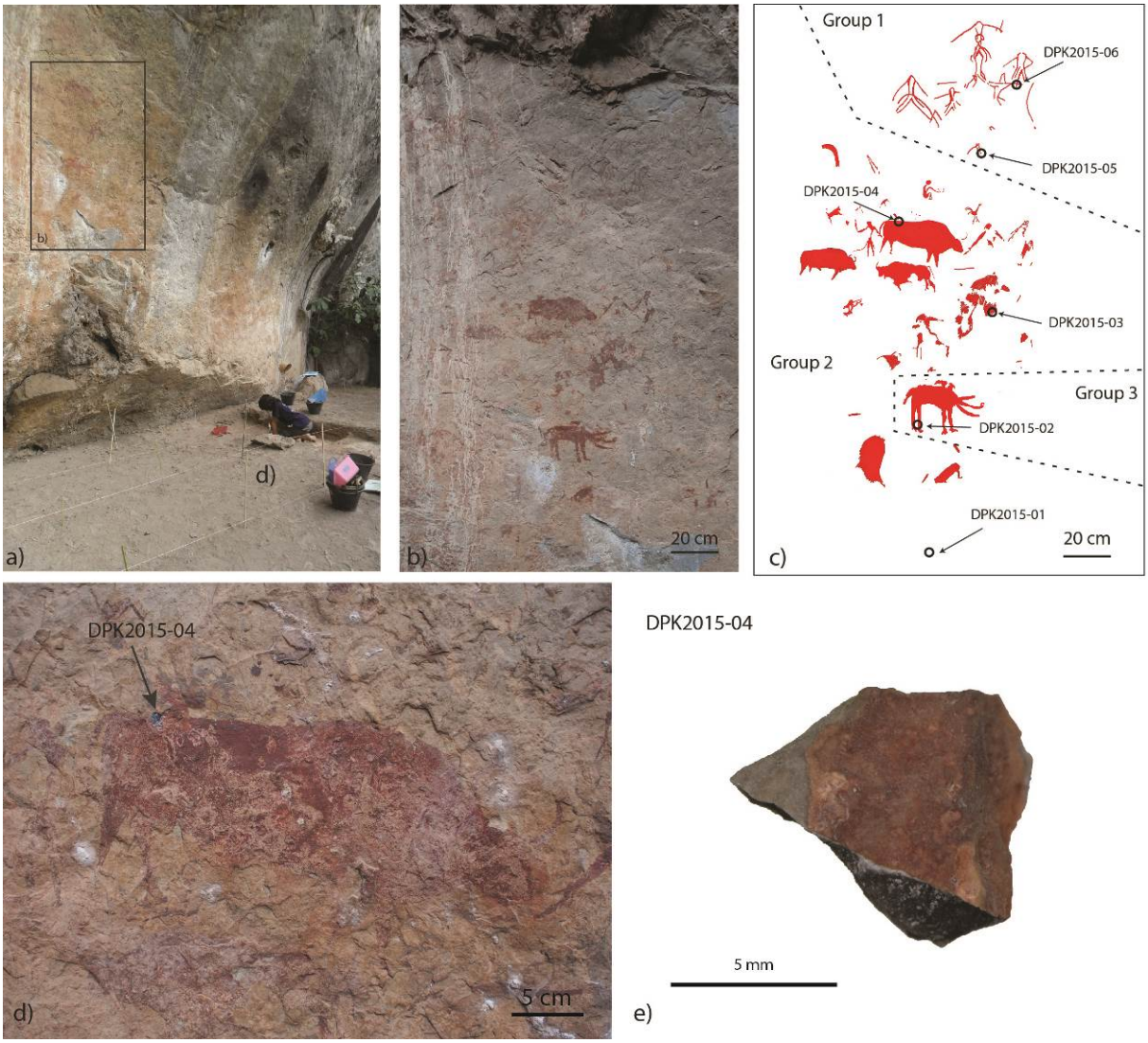

Fig. 3. a) Photograph of the painted wall at Doi Pha Kan during excavations; b) Detail photograph of the paintings (the colors of the photograph have been modified to ensure clarity of the image); c) Drawing of the paintings indicating the groups established from stylistic characteristics and sampling locations; d) Photograph of the bovid in the center of the panel and the location of sample DPK2015-04; e) Close-up photograph of sample DPK2015-04.

2.3 Sample preparation and analyzes

Due to the nature of archaeological material, non-invasive techniques were used for raw pigments and artifacts covered by red residues. All samples were analyzed by micro-X-Ray diffraction (μXRD) and X-Ray fluorescence spectrometry (XRF). Following this first set of analyzes, three fragments of raw pigments were selected and analyzed by conventional X-Ray diffraction (XRD) on powder to obtain more precise information on their mineralogical composition.

Samples from the painted wall were prepared as polished sections for optical microscopy and scanning electron microscopy (SEM) as follows. The samples were embedded in a polyester resin (Brot) under vacuum using CitoVac system (Struers). Resin blocks were then cut and pre-polished using Accutom-100 system (Struers) and then polished using Saphir 520 system from

Escil. A first polishing attempt was made using water-based diamond suspensions. This preparation causes some damage to the most superficial layers of the samples, by dissolving some of the more soluble minerals. A second preparation set was performed using an alcohol-based suspension causing less damage, although some cracks occured at the interface of the bedrock and upper layer. These cracks are easily recognizable by a green or blue coloration due to alcohol discoloration of the polishing cloths. However, the extent of these stains is limited and and observations can still be made in the preserved areas .

2.3.1 X-Ray fluorescence spectrometry (XRF)

Elemental analyzes were carried out using an Elio portable X-Ray fluorescence spectrometer developed by XGLAB. This system is composed of a X-ray source based on a Rh anode operating at a voltage between 10-50 kV and a current up to 200 µA for a maximal power of 4 W, and a Silicon Drift Detector with an active area of 25 mm^2. The source emission is collimated creating an analysis spot diameter of 1.2 mm on the sample at a working distance of 1.4 cm. Analyzes were performed at 40 kV and 100 µA, with an accumulation time of 300 s. Spectra were treated using PyMca software to calculate elemental concentrations from fundamental parameters (Solé, et al., 2007). Before being applied to DPK material, this treatment was tested on international geostandards from SARM (CRPG UMR 7358 CNRS-UL) to determine the accuracy of elemental concentrations calculated. Comparisons between the reference composition and concentrations obtained by XRF for four geostandards (DR-N, BX-N, CHR-Pt+, UB-N) are presented in Table 2. to estimate the chemical composition of samples and allow samples to be compared.

2.3.2 X-Ray diffraction (XRD) and micro-X-Ray diffraction (µXRD)

Blocks of raw materials displaying traces of human activities were analyzed exclusively by non-invasive micro-X-ray diffraction (µXRD). A selection of raw pigment samples was also analyzed by conventional X-ray diffraction (XRD).

Micro-X-Ray diffraction was performed using a system developed at the Laboratoire d'Archéologie Moléculaire et Structurale (SU-CNRS) for portable applications. This system is composed of an X-ray source (Xenocs) producing a quasi-parallel and micro-focused copper monochromatic beam (Cu-kα anode (λ = 0.15406 Å) operating at 50 kV with a beam spot size of 200 µm in diameter on the sample. Measurements are performed non-invasively by positioning the sample at the grazing incidence of the X-ray beam and recording the diffraction pattern in reflection mode. The diffraction patterns collected for 5 min on an imaging plate are read using Mini Plus VisaScan (Dürr Dental), and transformed to diffractograms using Fit2D software (ESRF). The system records diffractograms over a 10 ° to 50° 2θ range to characterize the most common minerals, even if some clay minerals cannot be identified reliably. For this reason, three samples of raw pigments (E4-286, E5-B1 and G6-32) were analyzed by XRD to determine their mineralogical composition, especially for clay minerals. After grinding of few mg, XRD was carried out on a silicon zero diffraction plate with a D2 phaser (Bruker) diffractometer equipped with a Cu-kα anode (λ = 0.15406 Å) operating at 30 kV and 10 mA. Diffractograms were collected over $3° < 2\theta < 65°$ with a step increment of 0.04° and acquisition time of 0.2 sec by step.

2.3.3 Raman spectroscopy

Cross sections were analyzed by Raman spectroscopy to determine the mineralogical composition of crust and pigment alterations. Analyzes were carried out using a Labram HR800 spectrometer (Horiba Jobin Yvon) using the 514 nm excitation of an Ar^+ laser source. The Rayleigh line is filtered due to ultra narrow band Notch BragGrate filters. Areas of interest were located and analyzes were made through a x100 objective giving a focused laser of about a 1 µm spot. Laser power was adjusted to around 80 µW at the sample. Raman spectra were collected between 20 and 1850 cm^{-1} with a spectral resolution of 2 cm^{-1} using a 1800 lines/mm grating. Spectra were corrected for edge filter ripples (Casadio, et al., 2016) and baselines were corrected using Labspec software (Horiba Jobin Yvon) to substract the fluorescence background. The main mineral components were determined using the RRUFF database and CrystalSleuth software (Lafuente, et al., 2015).

2.3.4 Scanning Electron Microscopy and Energy Dispersive X-ray Spectroscopy (SEM-EDS)

Following Raman analyzes, polished sections were carbon coated and studied using a Tescan VEGA II LSU scanning electron microscope (SEM) in high vacuum mode. The sample textures were observed in backscattered electron mode (BSE) and elemental analyzes were performed using an Energy-Dispersive Spectroscopy (EDS) detector (SD3 Bruker) at an accelerating voltage of 20 kV.

3/ Results and discussion

3.1 Colored rocks and ochres from the archaeological grave dpk E-5

Table 3 reports the mineral phases identified and the major, minor and main trace elements detected. The composition of the pendant (samples E5-286) and faceted colored artifact (E5-15) is dominated by quartz (SiO_2), and associated with calcite ($CaCO_3$) for the pendant. This is confirmed by the high concentration of Al (21 wt% for E5-286 and 20 wt% for E5-15) and Si (44 wt% for E5-286 and 40 wt% for E5-15), and low content of Fe (6 wt% for E5-286 and 14 wt% for E5-15) measured by XRF. The Al in these samples suggests the presence of aluminosilicates undetected by µXDR. Concentrations of Fe are low for these samples; the associated minerals revealed by XRD are only traces of goethite ($FeO.OH$) and/or hematite (Fe_2O_3). These analyzes confirm that these two artifacts were made with hued rocks rather than blocks of raw pigments.

Samples visually identified as powder and fragments of ochre are mainly composed of hematite, which is associated with variable amounts of quartz, a clay phase, and some goethite for a few samples (DPK-E4-286 and DPK-E5-B1). The identification of clay by µXRD was limited by the 2θ range of the set-up used. However, the µXRD pattern suggests the presence of kaolinite that was confirmed by XRD analyzes performed on three samples of ochre. In addition, calcite was identified for sample E4-286. Elemental compositions determined by XRF highlight a high content of iron oxide associated to Al and Si, which is consistent with mineralogical analyzes. K and/or Ca in lower concentrations were also detected for several samples. The elemental

composition is variable and Fe contents fluctuate from 20 wt% to more than 60% wt%. The ochre fragment G6-32 displays a very different mineralogical composition since the phase of hematite is associated with goethite, calcite, quartz and kaolinite. Some traces of jarosite ($KFe_3(SO_4)_2(OH)_6$) and alunite ($KAl_3(SO_4)_2(OH)_6$) were also detected. The presence of jarosite and alunite explains the high amount of K and S detected in this sample. Analyzes by µXRD suggests the presence of halite that could explain Cl concentrations, but this mineral was not found in XRD. This suggested a heterogeneous and local presence of halite or its deposits on the surface of the block.

With the exception of the G6-32 sample, all the samples have Fe contents correlated with As (r^2 = 0.75) and to a lesser extent with Cl (r^2 = 0.6). The trends observed between As and Fe for ochre powders are slightly different (samples E5-B1 and E4-286; Fig. 4). However, these high levels of As, and the association of Cl and As to the iron oxide phase suggest a common geological origin.

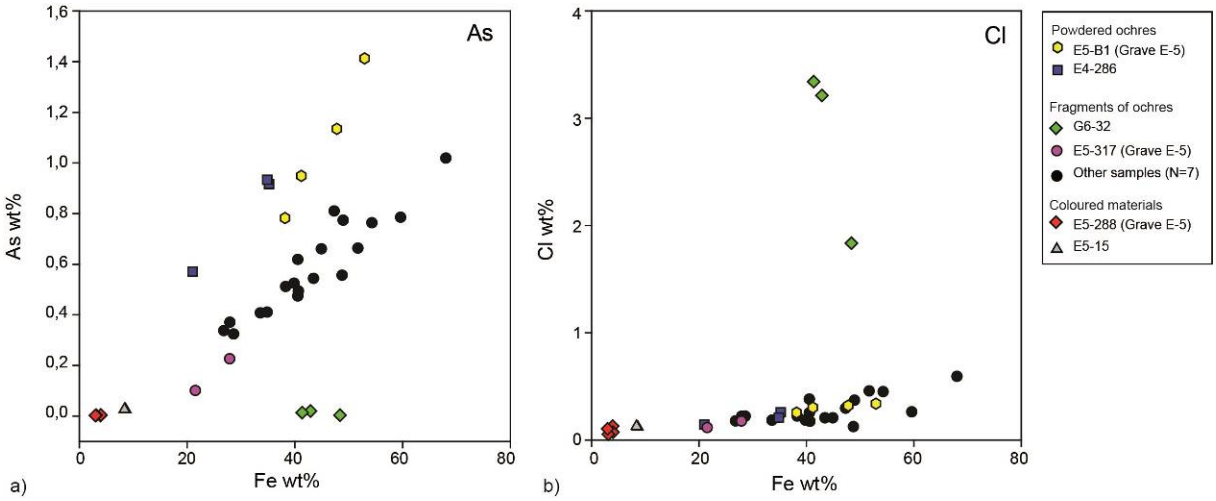

Fig. 4. Relationship between Fe content and (a) As content (b) Cl content measured by XRF for colored rocks and ochres. All duplicate measurements are plotted for each sample.

3.2 Pigments on artifacts and wall fragments from archaeological levels

Pigments present on several supports discovered in the DPK archaeological context were also analyzed by XRF. Unfortunately, the pigment covering the hole of the perforated stone was not suitable for XRF analysis due to the geometry of the analytical head, but µXRD confirmed the presence of hematite. For these samples, the distribution of ochre deposits is very heterogeneous and it was not possible to identify areas large and thick enough to avoid the simultaneous XRF analysis of pigment and its support. A quantitative analysis was impossible but a qualitative comparison between the pigment layer and its support can provide valuable information on the nature of the ochre. As shown in Fig. 5a and Table 3, the ochre layer on the painted calcareous pebble is characterized by a high Fe content associated with As. It is also the case for the pigment on the three fragments of painted wall (flakes) excavated from the archaeological layer (e.g. for sample I4-256 in Fig. 5b) and for all the artifacts covered by pigment deposits. When possible, sediment encrusted in cracks or covering samples were analyzed. These analyzes indicated the absence of As in the sediment, demonstrating that its presence in the pigments does not result from a post-depositional process and a contamination

from a sediment containing As. The elemental composition of hematite-based pigments found on the archaeological artifacts and painted wall flakes is very homogeneous and similar to the composition of ochre fragments and powders coming from the grave dpk E-5 and surrounding sediment.

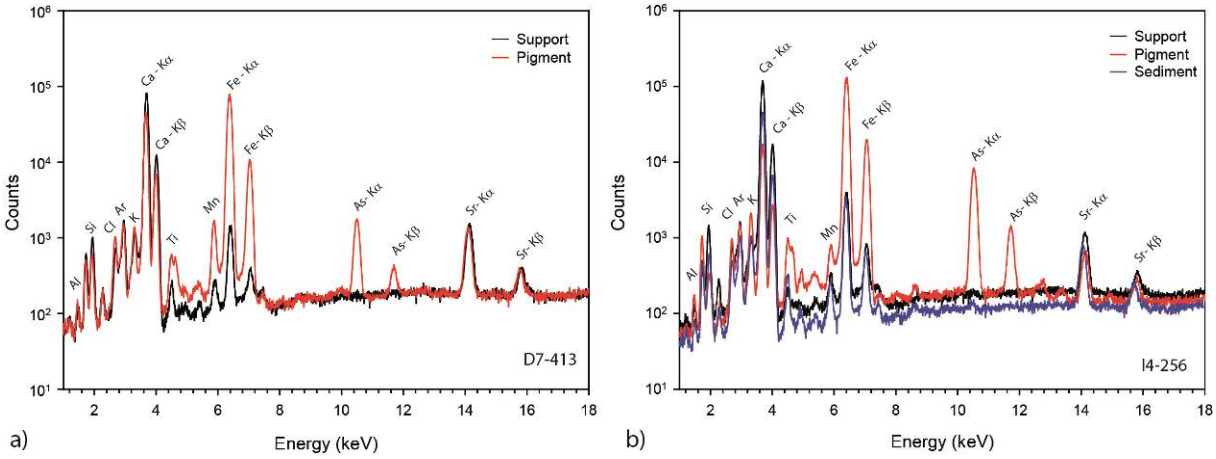

Fig. 5. XRF spectra comparisons for pigment (red line), substrate (black line) and sediment (blue line) for two samples : (a) a painted calcareous pebble (D7-413) and (b) a painted wall flake (b – I4-256)

Although a detailed geological survey to identify the potential sources of iron-rich rocks has not yet been undertaken, the information obtained from the raw pigment analysis can provide clues to their origin. Indeed, various studies have shown that the use of elemental compositions can discriminate between different sources of ochres and iron-rich rocks (Beck, et al., 2011, Dayet, et al., 2016, Zipkin, et al., 2015, Beck, et al., 2012, Mathis, et al., 2014, Popelka-Filcoff, et al., 2008). These studies were carried out using various analytical techniques, such as ion beam analysis, neutron activation, and as in this study by X-Ray fluorescence spectrometry.

The presence of As in DPK pigments supports the hypothesis of a local origin of the material. Indeed, a few kilometers from the DPK site lies the Mae Moh mine, which is the largest open-cast mine in Thailand. Several levels of lignite coal deposit are exploited, coming from sediments of the Tertiary Mae Moh Basin (Morley and Racey (2011) ; Jitapankul, et al. (1985) in Ratanasthien, et al. (2008)). The geological layers interlayered between lignite deposits are mainly dominated by siltstone and claystone, and some geological layers, richer in iron oxides, have been identified within the stratigraphic sequence of the basin (Vichaidid, et al., 2012). Moreover, some lignite layers are characterized by a high As content with concentrations that can reach more than 500 ppm (Bashkin and Wongyai, 2002). Iron oxide minerals, such as hematite, have a significant capacity for arsenic sorption (Mamindy-Pajany, et al., 2009, Giménez, et al., 2007). Thus, the presence of arsenic in iron-based raw pigments could result from iron oxide enrichment of iron-rich rocks from the groundwater at a regional scale, or more locally within the stratigraphic levels of the Mae Moh basin.

Regarding the mineralogical composition of sample G6-32, a fragment of raw pigment, jarosite is a secondary mineral that forms crusts and coatings on the surface of iron ores or in the cracks of associated rocks. It is present, associated with alunite, in oxidation zones of iron sulfide deposits, in particular of pyrite (Palache, et al., 1951). It is also a common mineral in sulfate-acid soils linked to pyrite oxidation (Vieillefon J., 1973). These soils are frequent in Thailand and especially

in the Chao Phraya basin, which extends from the Lampang region in the north to Bangkok in the south (Marius C., 1981). The presence of pyrite is notably reported in several layers of the Mae Moh basin (Ratanasthien, et al., 2008). These elements also give evidence for a local or regional origin for sample G6-32.

3.3 **Pigments from wall samples**

Before preparing the polished sections, samples were photographed and observed under a stereomicroscope. Areas of interest were observed using a Hirox digital microscope with magnifications from x20 to x600. An alteration crust covering the pigment layer was observed (Fig. 6). In the thinnest parts of the deposit, this is almost transparent and the underlying pigment layer is still visible (Fig. 6a). However, in the thicker parts, it takes the appearance of white or gray deposits with large crystals (Fig. 6b). Some small black grains are trapped in this upper crust layer, suggesting carbonized organic matter fragments.

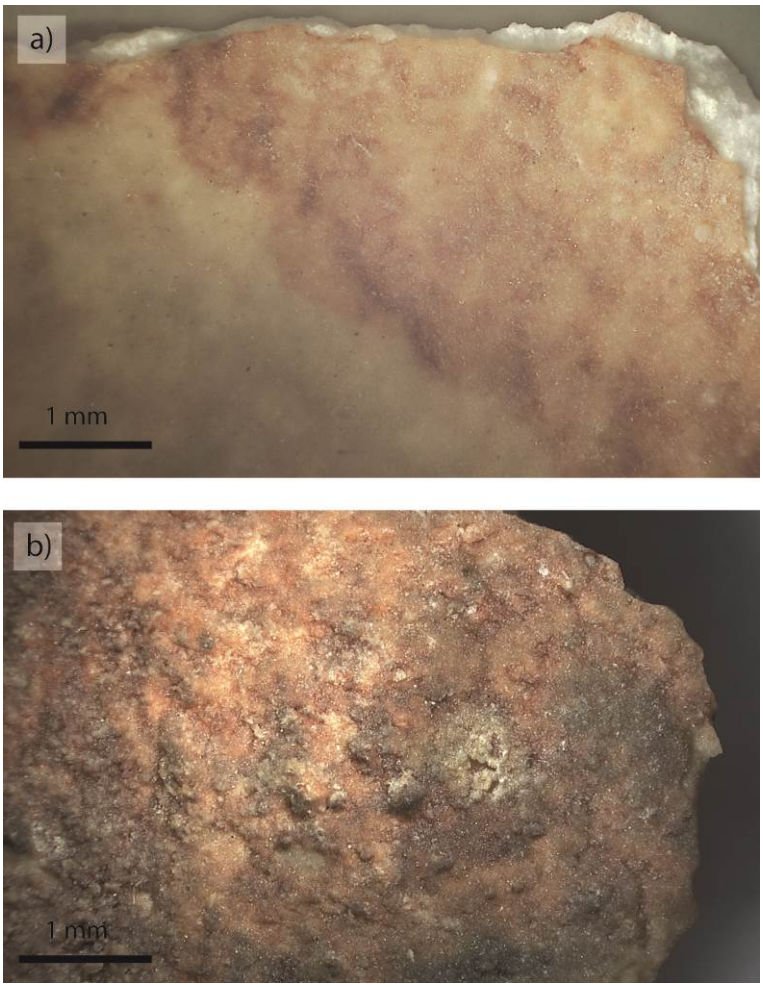

Fig. 6. Photographs illustrating the alteration crusts covering the pigment on samples (a) DPK15-5 and (b) DPK15-06

3.3.1 Rock substrate

SEM micrographs of the rock supporting the painting display a matrix composed of white angular grains including some grey grains (Fig. 7a). Elemental analysis by EDS and Raman spectroscopy are consistent and identify dolomite grains ($CaMg(CO_3)_2$) in a calcite matrix ($CaCO_3$). The outer part of the bedrock is affected by alterations that have led to cracking and a partial dissolution of the limestone. This dissolution affects the grains from their boundaries and then increases porosity between them and a disaggregation of the most superficial limestone grains. At the outer limit of the bedrock, these porosities are filled by alteration deposits.

3.3.2 Superficial alteration crusts

Observations of polished sections show that the thickness of the crust layers on the surface of the samples is highly variable and can range from 10 µm for sample DPK15-06 to more than 150 µm for DPK15-01 (see sample locations in Fig. 3). The characteristics of the alteration crusts and their composition are summarized in Table 4.

Fig. 7 shows a selection of representative Raman spectra acquired on the alteration crusts. The surface alteration layer is mainly composed of gypsum ($CaSO_4$, $2H_2O$) identifiable by the main band at 1009 cm^{-1} (Bell, et al., 1997), and whewellite, a calcium oxalate ($Ca(C_2O_4)$, H_2O), identifiable by bands at 1490, 160, 987 and 503 cm^{-1} (Frost, 2004). These two phases were identified for almost all Raman spectra obtained on this alteration layer. These two minerals are less frequently associated to calcite ($CaCO_3$) with its main band at 1087 cm^{-1} (Bell, et al., 1997). The presence of an anatase peak (titanium dioxide, TiO_2) at 143 cm^{-1} (Middleton, et al., 2005) and broad bands of amorphous carbon at 1608 and 1356 cm^{-1} (Bell, et al., 1997, Pagès-Camagna, et al., 2004) were also detected. The presence of black carbon, probably charcoal, could explain the nature of the black grains observed by optical microscopy.

For sample DPK15-01, from an area without painting, SEM observations of the alteration layer highlights the presence of large crystals whose size exceeds 20 µm in the most superficial part of the crust (Fig. 7a). Elemental analyzes performed by EDS show that these crystals are mainly composed of Ca, S and O corresponding to gypsum identified by Raman spectroscopy. The underlying layer presents some diffuse areas ranging from light grey to dark grey in BSE pictures, including white particles up to about 5 µm in diameter. The composition of this layer is very heterogeneous: darker areas are mainly composed of oxalates or calcium carbonates associated with aluminosilicates in variable concentrations. Light grey areas are composed of Ca, S and O, highlighting the presence of gypsum. Small light grey and white particles in this matrix have various mineralogical compositions. As seen on Fig. 7b, the composition of these particles suggests the presence of an apatite like mineral ($Ca_5(PO_4)_3$), anatase (TiO_2) and quartz (SiO_2). Baritine ($BaSO_4$) was also detected in sample DPK15-02 by SEM-EDS.

The two major mineral phases identified in the superficial alteration layer are whewellite and gypsum. These minerals have been commonly found in alteration crusts on a large variety of rock supports including sandstone, granites, and in this case limestone (Scott and Hyder, 1993, Watchman, et al., 2001, Russ, et al., 1999). Whewellite mainly forms from the interaction between calcium and oxalic acids released by the biological activity of fungi, bacteria, algae or lichens (Russ, et al., 1999, Roberts, et al., 2015, Ford, et al., 1994, Del Monte, et al., 1987).

Gypsum formation on stone is a well-known process which alters historical monuments in urban and polluted environments. It results from the reaction of atmospheric sulfur dioxide with Ca from the stone substratum to form a calcium sulfate crust (Del Monte and Sabbioni, 1984, Siedel, et al., 2010). The physicochemical and biological processes leading to the formation of such minerals in natural environments are less documented. In contrast to buildings, the most proposed source for gypsum deposit in the rock art context is flowing groundwater (Russ, et al., 1999, Roberts, et al., 2015). However, several studies have shown that bird and bat droppings generate a low pH solution with a high ion content that can form a large variety of salts, including gypsum and oxalates (Siedel, et al., 2010, Gömez-Heras, et al., 2004). However, the presence of large deposits of gypsum raises questions since this mineral is a soluble salt precipitating in dry conditions and generally associated to surfaces protected from rain-washing (Chalmin, et al., 2017a). The small overhang over this part of the painted panel seems to protect it from direct rain and prevents gypsum solubilising during rainy periods.

Bird and bat droppings are also particularly rich in phosphate and their degradation by micro-organisms could explain the presence of calcium phosphate minerals identified by SEM-EDS (Watchman, et al., 2001). Regarding quartz and titanium oxide grains, they most likely originate from the transport of detrital material by water run-off or aeolian transport of dust.

Although it is difficult to accurately identify the processes at the origin of these mineral deposits on the painted panel of DPK, they lead to an irremediable alteration of the paintings. The structure observed by SEM on sample DPK15-01 (Fig. 7) at the junction between the substrate and the alteration crust may have resulted from the partial dissolution of limestone grains, due to low pH conditions, followed by the growth of gypsum and oxalate minerals that disaggregate the grains in the uppermost layer of the rock. This process of gypsum crystal growth in a porous matrix has been identified for sandstone (Watchman, 1990) and limestone (Gömez-Heras, et al., 2004) as a source of rock spalling. This phenomenon is clearly observed on the walls of the DPK rock-shelter and has already led to many parts of the figures being removed.

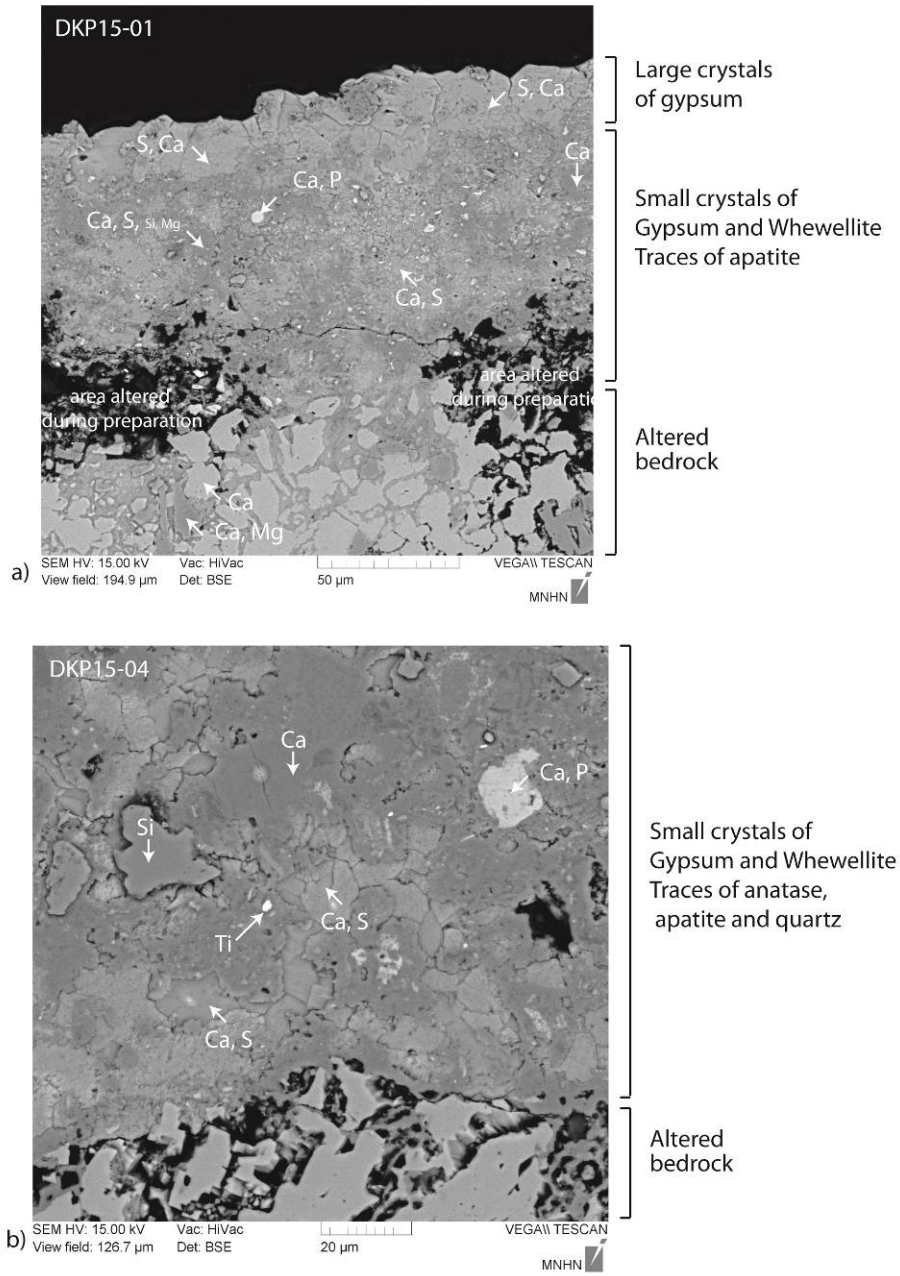

Fig. 7. SEM-BSE micrograph and results of the EDS elemental analysis performed on the alteration crust of sample DPK15-01 collected outside the painted area on the DKP panel. a) General view of the alteration crust on the calcareous substrate and b) Details of the mineral phases identified by EDS analysis : gypsum (Ca, S), whewellite (Ca), quartz (Si), anatase (Ti) and apatite-like mineral (Ca, P).

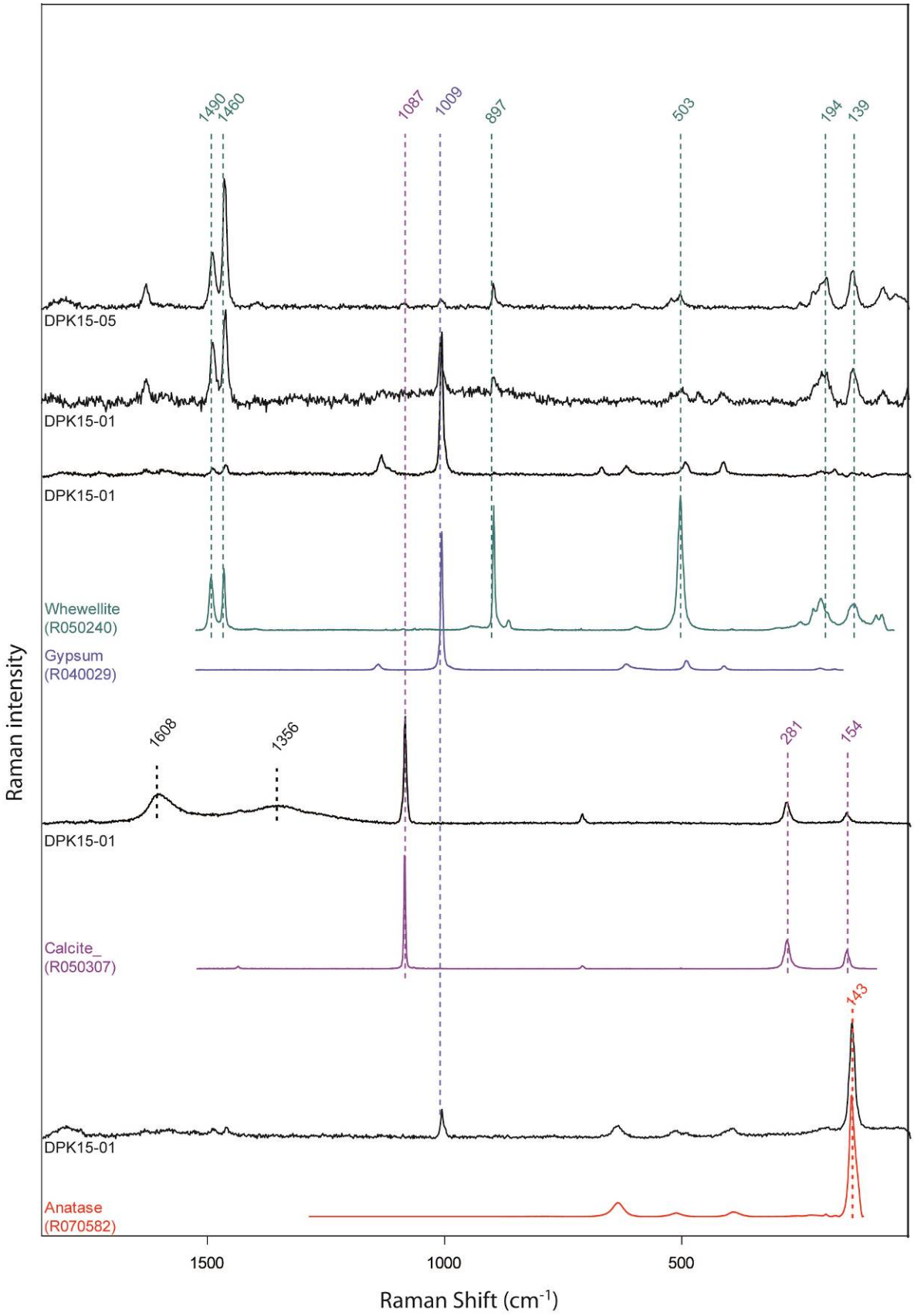

Fig. 8. Representative examples of Raman spectra (baseline corrected) of the various mineral phases identified in the alteration crusts with the corresponding reference spectra from the RRUFF database.

3.3.3 Pigment layers

Pigment layers observed from rock painting samples show high variability, both in terms of their thickness, composition and position compared to the surface alteration crust. Table 4 summarizes the results obtained from SEM observations and elemental analyses by EDS.

The sample DPK15-02 presents a relatively thick painting layer on the top of the alteration crust (Fig. 9a, b). SEM observations combined with elemental EDS analysis show that this layer is composed of iron oxide grains (white grains on Fig. 9c) measuring up to 5 µm and associated with aluminosilicates. These aluminosilicates are in the form of small grains of about 10 µm in length (Fig. 9c). Their laminated structure and the Al:Si ratio close to 1 suggest the presence of kaolinite ($Al_2Si_2O_5(OH)_4$). Some quartz grains can be found locally within the pigment layer, as well as gypsum and whewellite.

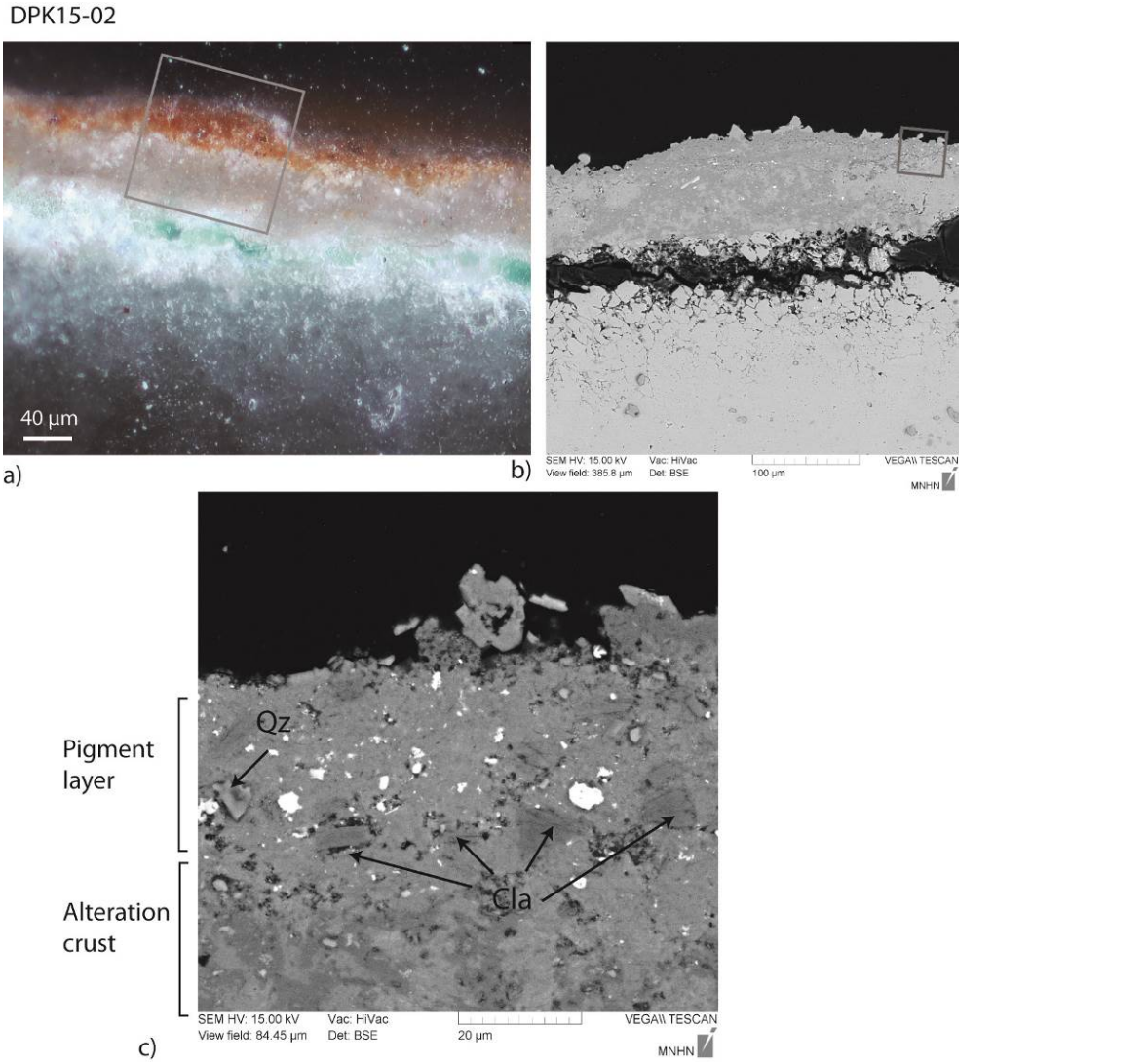

Fig. 9. a) Optical microscopy image of the pigment layer in the thin section of sample DPK15-02. b) and c) SEM-BSE micrographs of the superficial crust and pigment deposit. Quartz grains (Qz) and clay aggregates (Cla) are indicated on the micrograph and white grains correspond to iron oxide c).

For sample DPK15-03, the composition of the pictorial layer is similar to that of the sample DPK15-02 with a mixture of iron oxide and aluminosilicates. However, its pigment layer is characterized by a higher frequency of quartz grains than for the pigment layer of sample DPK15-02 (Fig. 10).

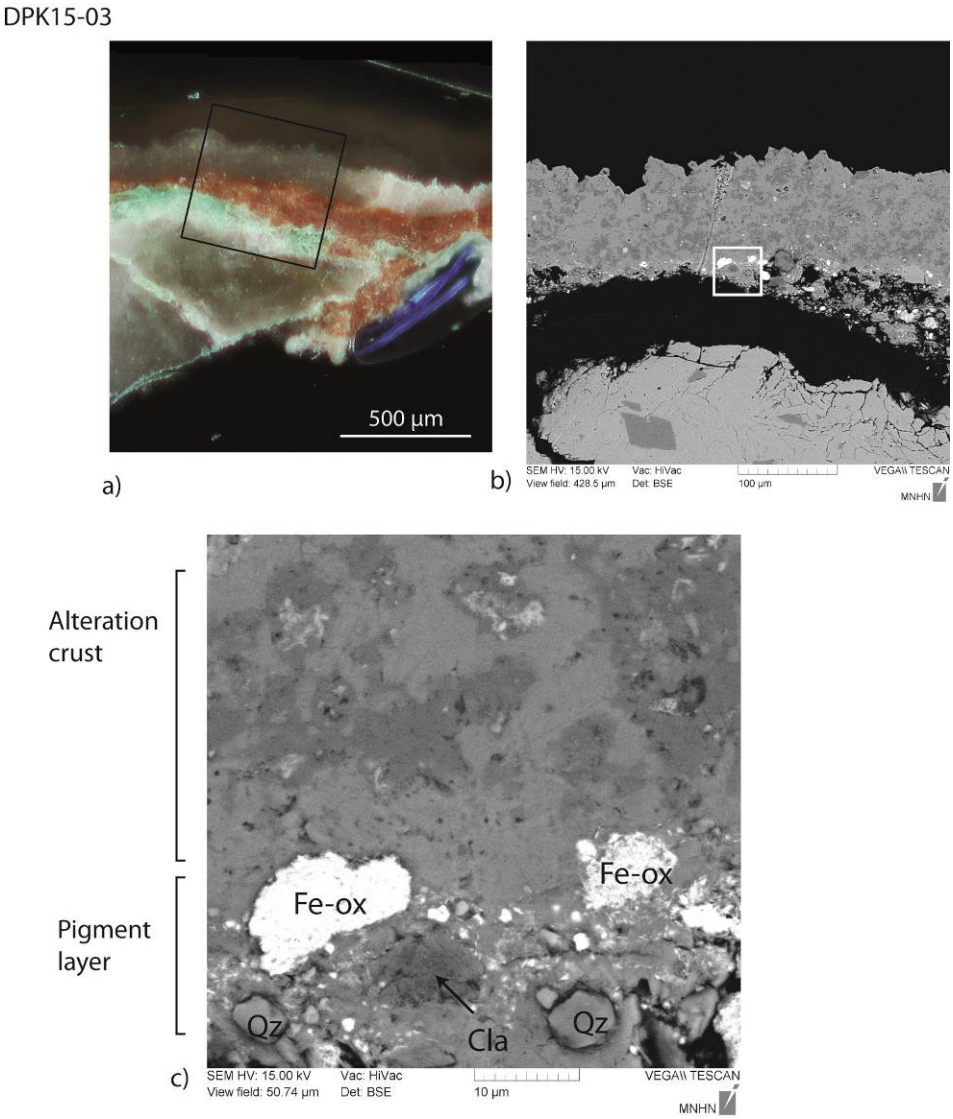

Fig. 10. a) Optical microscopy image of the pigment layer on the thin section of sample DPK15-03. b) and c) SEM-BSE micrographs of the superficial crust and pigment deposit. Iron oxide (Fe-ox) and quartz grains (Qz) and clays aggregates (Cla) are indicated on micrograph c).

Sample DPK15-04 comes from an area of the panel where two pigment layers have overlapped: the lowest layer corresponds to the red bovid and the superficial layer to a small spot with an orange-red hue.

These two layers can be easily observed by optical microscopy on a polished section (Fig. 11a). However, these layers are more difficult to visualize in SEM-BSE images due to the scattering of the rare and small iron oxide particles (white grains on Fig. 11b). The superficial layer is composed of a fine matrix of aluminosilicates and iron oxides. This layer is extremely thin unlike

the lower layer which seems thicker. The lower layer is also characterized by the presence of quartz grains. Elemental mapping (Fig. 12) performed by SEM-EDS highlights the different compositions of these two layers: the alteration crust is mainly composed of Ca and S, and the pigment layers by Fe, Al and Si, with a higher proportion of Si in the lower layer.

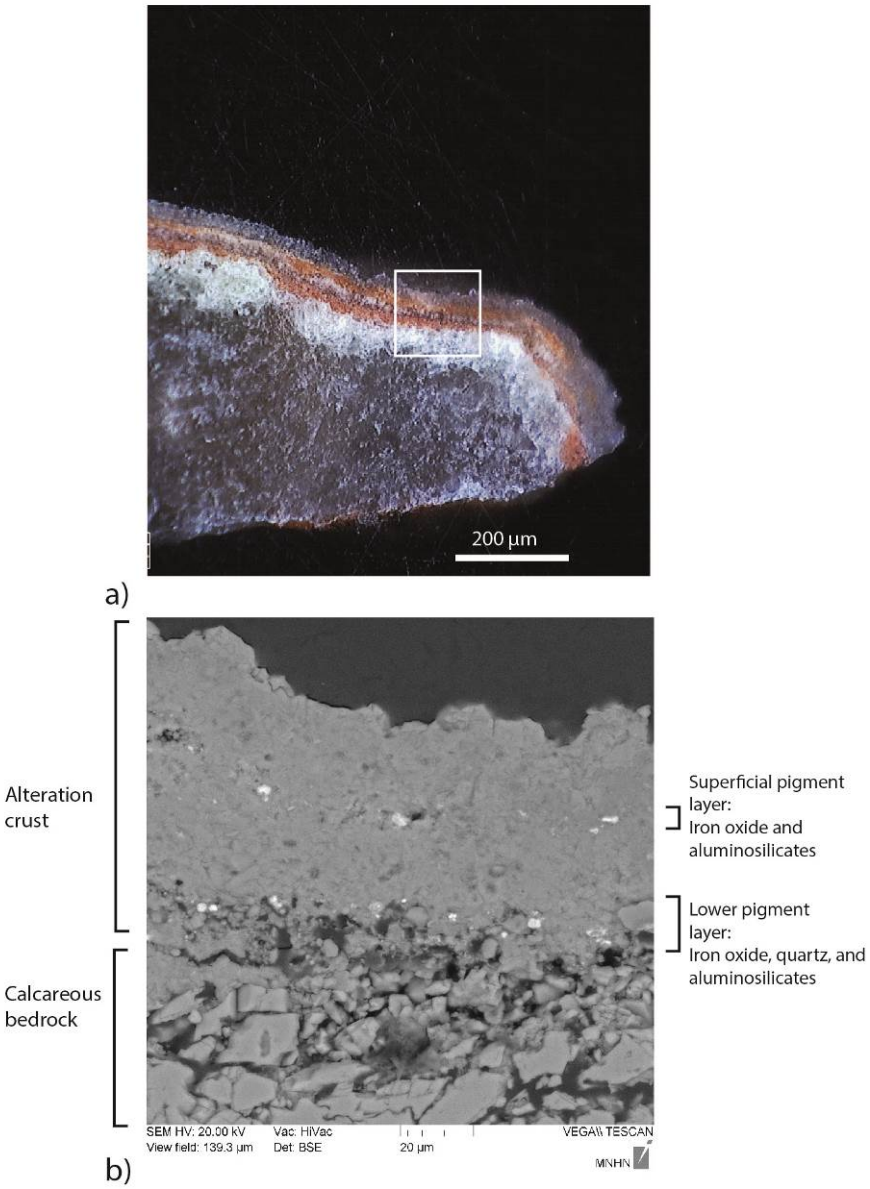

Fig. 11. a) Optical microscopy image of the pigment layer on the thin section of sample DPK15-04. b) SEM-BSE micrograph of the superficial crust and pigment deposit.

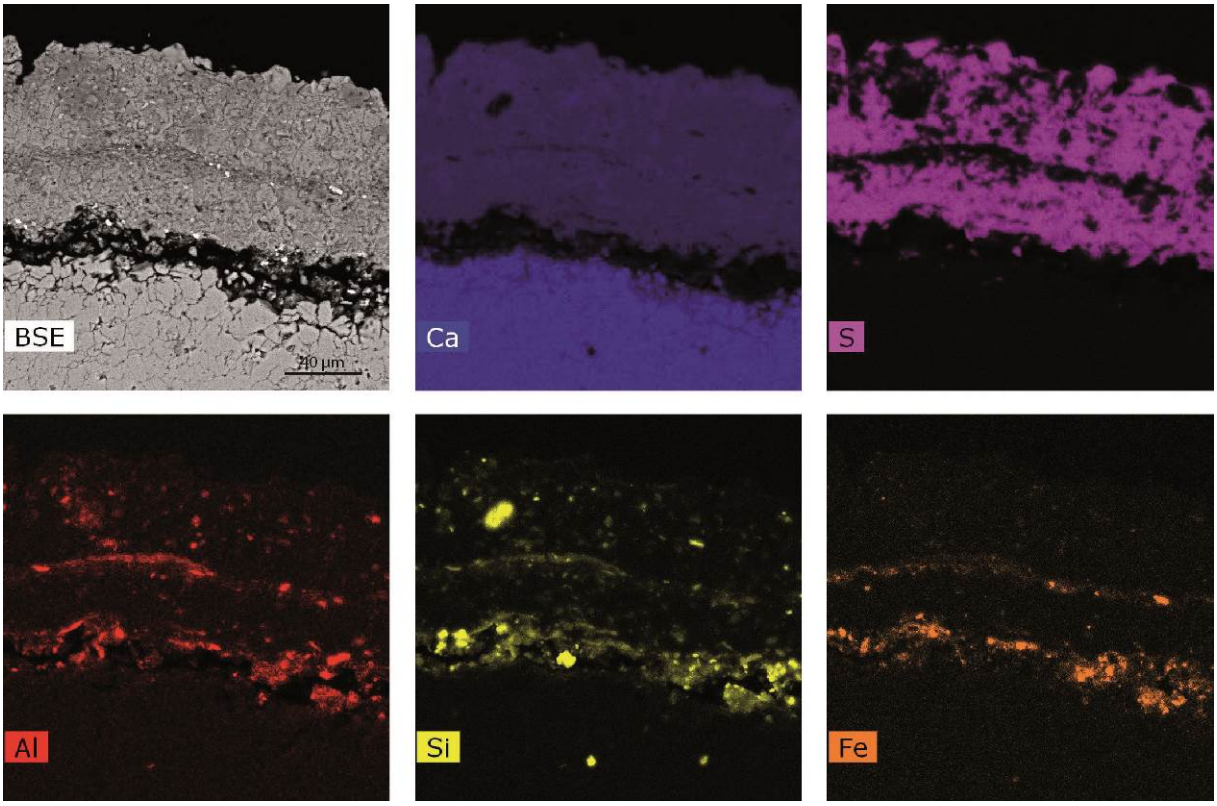

Fig. 12.: SEM-BSE micrograph of the superficial layer of the polished section of sample DPK15-04 and the elemental distribution of Ca, S, Al, Si, and Fe (EDS maps).

Sample DPK15-05 has a thin pigment layer located at the base of the alteration crust, almost in contact with the calcareous support (Fig. 13). This layer is very thin, continuous, and consists of very small iron oxide particles (mostly <1 µm). These particles are associated with a fibrous matrix of aluminosilicates, and with alteration products in the rest of the superficial layer. Given the type of SEM system used and the nature of the samples studied, the volume of the electron/material interactions did not obtain a spot size small enough to exclusively analyse the iron oxide phases of the pigments without any contributions from the other compounds.

The polished section of sample DPK15-06 shows a pigment layer with a thickness between 10 and 20 µm. However, small crevices in the substrate can lead to the presence of pigment clusters that may exceed a thickness of 100 µm (Fig. 14a). The EDS analyzes and SEM observations show that this cluster consists mainly of a mixture of iron oxide grains smaller than 1 µm in a fibrous clay matrix (Fig. 14b, c). However, iron oxide particles of larger sizes (>10 µm) were also observed (Fig. 14c). These particles were larger than those observed for the other samples, and an EDS analysis suggests the presence of As (Fig. 14d).

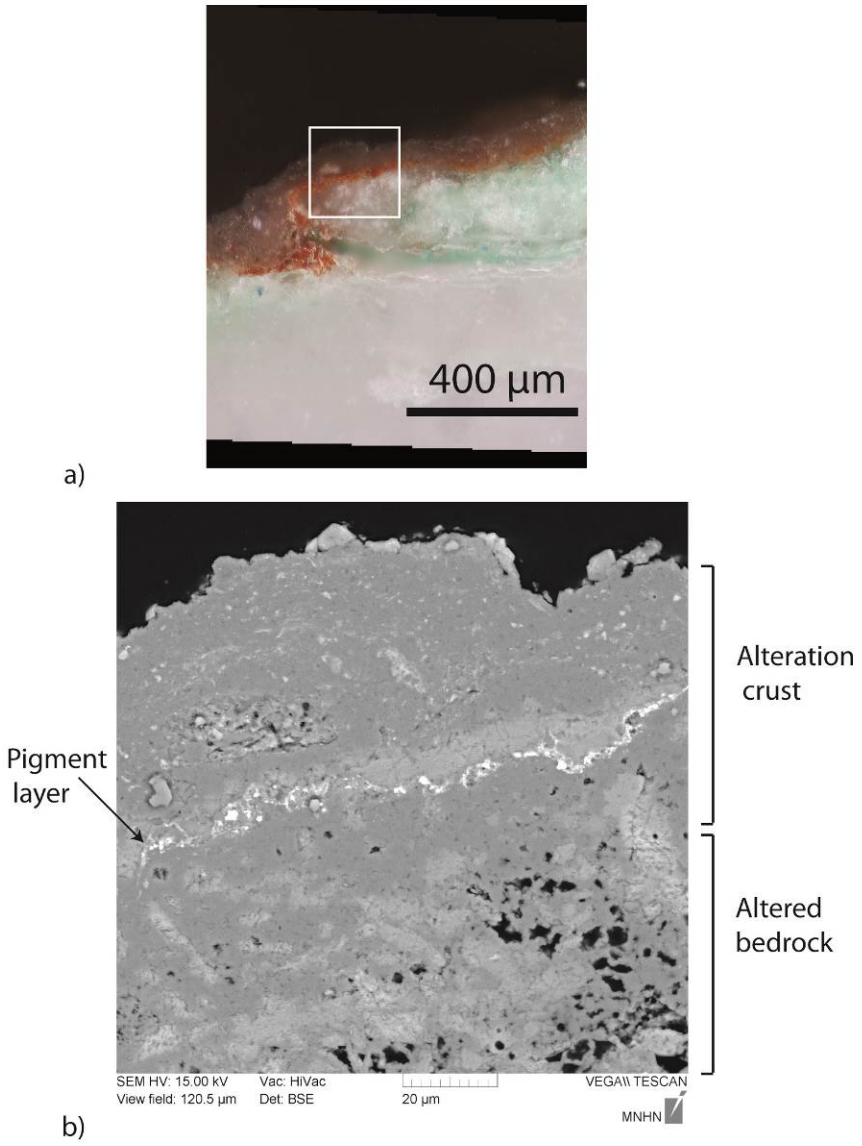

Fig. 13. a) Optical microscopy image of the pigment layer on the thin section of sample DPK15-05. b) SEM-BSE micrograph of the superficial crust and pigment deposit.

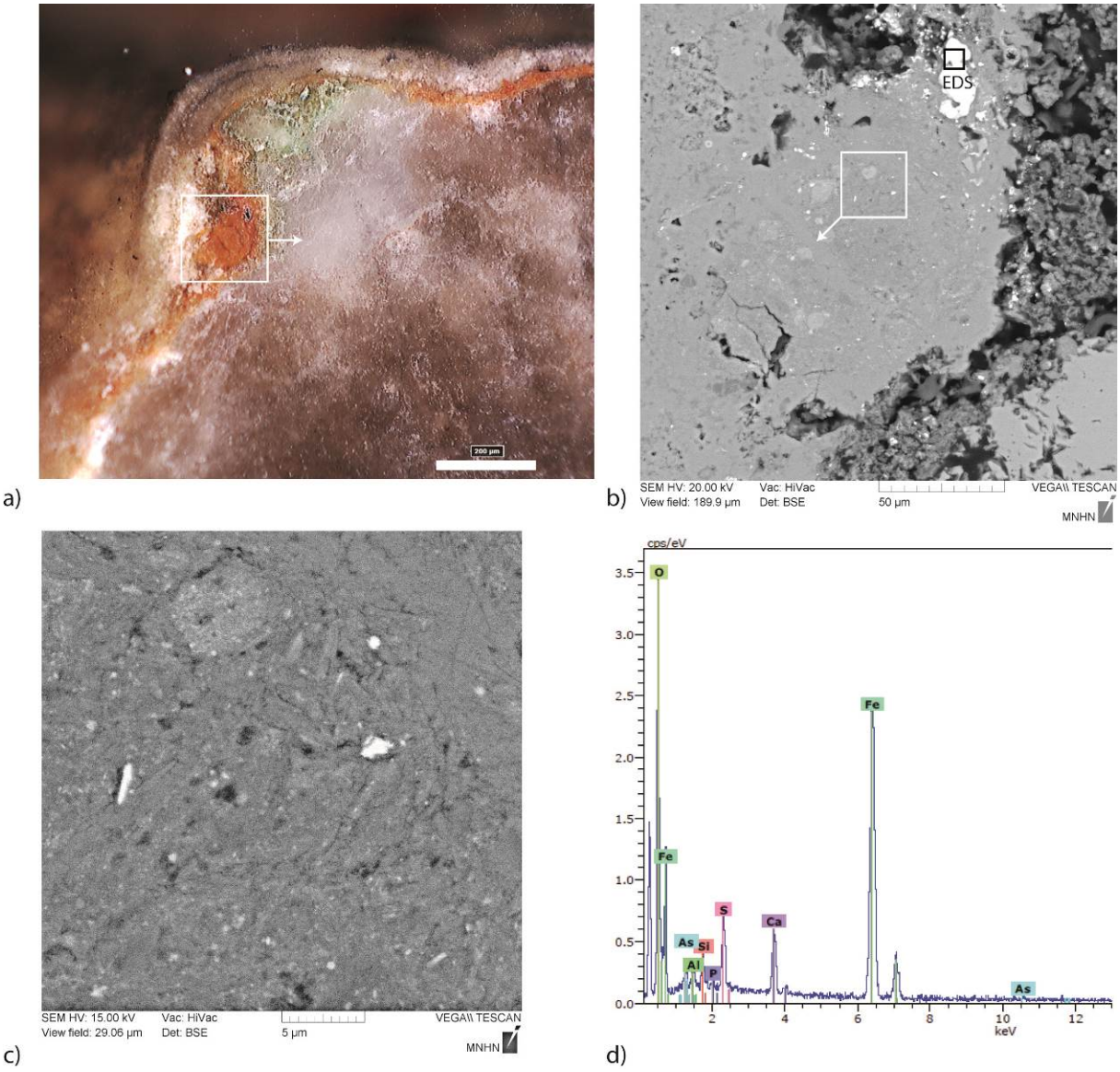

Fig. 14. a) Optical microscopy image of the pigment layer on the thin section of sample DPK15-06. b) and c) SEM-BSE micrographs of a pigment aggregate . d) EDS spectra for a large iron particle showing the presence of As as a trace element.

To confirm the presence of As in these samples from the painted wall, XRF analyzes were performed at the surface of the samples. Although quantitative measurements could not be conducted, the comparison of XRF spectra for the substrate and the painted surface shows chemical differences. The presence of As in pigments was confirmed by XRF spectroscopy. As shown in Fig. 15, the comparison of the elemental composition of pigment and rock substratum shows traces of As in samples DPK15-05 and DPK15-06. Peaks of As are lower than those collected by XRF for the pigment on wall flakes associated to burials (Fig. 5b; DPK-I4-256 and DPK-I3-425), but it is also the case for Fe peaks. Thus, it appears that pigments on DPK15-05 and DPK15-06 are thinner. This could be consistent with a better preservation of excavated samples, separated earlier from the wall and protected from erosion. No traces of As were detected by XRF spectroscopy in other samples on the painted wall.

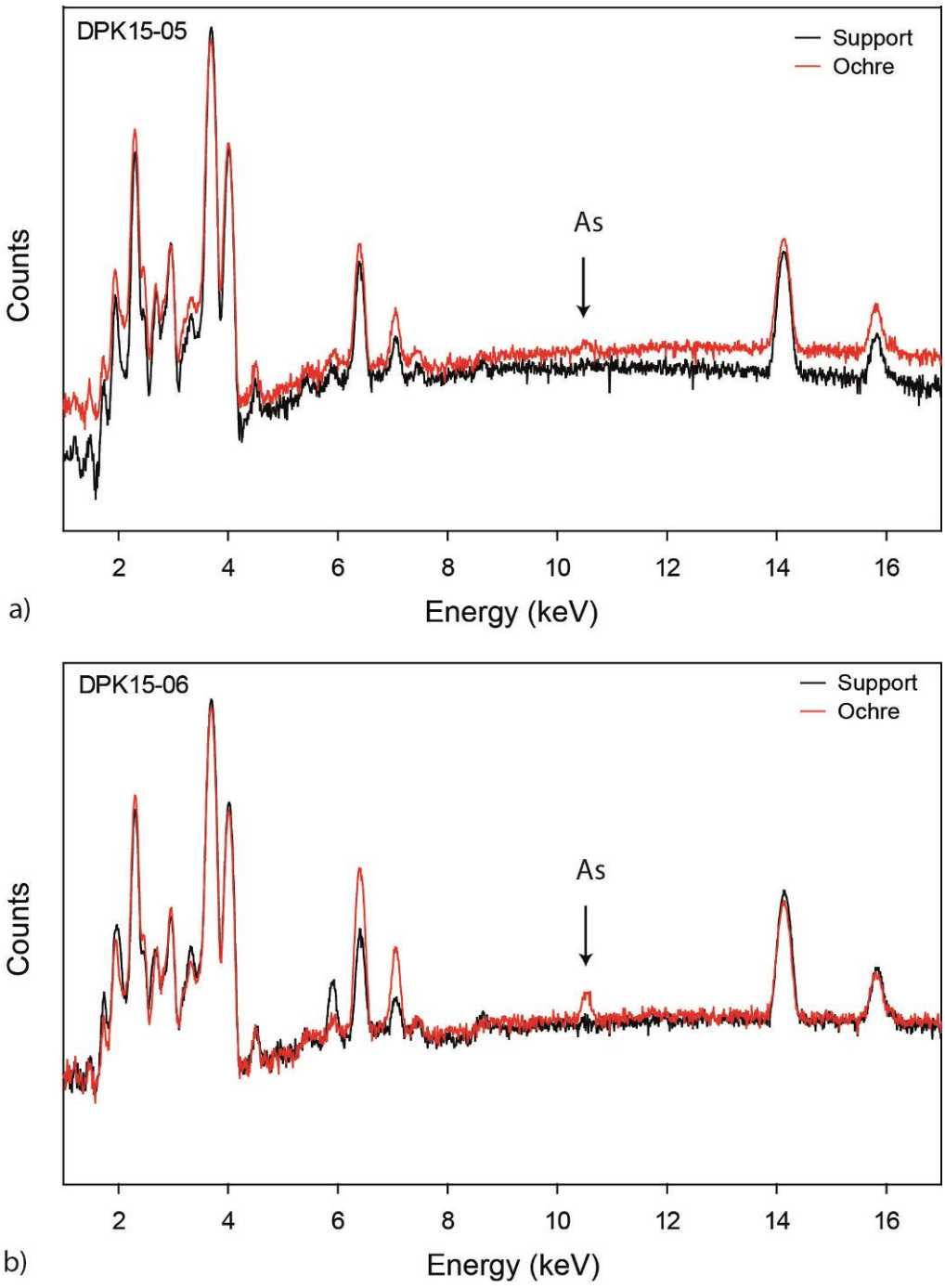

Fig. 15. XRF spectra comparison for the substrate (black line) and pigment (red line) for painted wall samples (a) DPK15-05 and(b)DPK15-06.

3.3.4 General discussion on raw materials and pigments used at Doi Pha Kan

The nature of the pigments used on the painted panel at DPK and their relative position within the alteration crusts provide information about the chronology of the production of these symbolic expressions. The analyzes conducted in this study do not completely identify the different phases of painting production, because of the limited number of samples that could be collected. However, at this stage of the study, three main groups of paintings can be identified from their composition and relative position on the substrate and alteration crust:

- Group 1: outlined anthropologic figures with pigments containing traces of As (DPK2015-05 and DPK2015-06).
- Group 2: a pastoral scene in the center of the panel (DPK2015-03 and DPK2015-04),
- Group 3: an elephant characterized by a pigment deposit on the surface of the alteration crust (DPK2015-02)

These three groups correspond with those previously based on stylistic criteria (Surinlert, et al., 2018, Surinlert, 2013) (Fig. 3). For samples whose pigments do not contain As (groups 2 and 3), two different compositions can be distinguished, based on their concentrations of quartz, aluminosilicates and iron oxides. However, such variations can be observed within the same geological formation and thus it is difficult to assure that these two types of pigments come from distinct geological sources.

The pigments present on painted wall fragments and the majority of archaeological artifacts displayed a similar elemental composition characterized by a high As content (more than 1%). This suggests a preferential exploitation of a given geological source, probably local, as evidenced by the high level of As in some geological formations near the DPK site.

Although the composition of raw pigments from the archaeological context is homogeneous, this is not the case for rock paintings. This suggests the differential availability and use of pigment resources for the various painting steps for the DPK panel.

The presence of As in geometric anthropomorphic figures indicates that these paintings were made with the same pigments as those used in the archaeological levels and excavated burials. The presence of pigment containing As on wall fragments found in the archaeological layer shows that this pigment was already used for painting during the Hohabinian period. Although this does not establish a direct link between burials and paintings, if some figures contemporary to the occupation layer have been preserved, it could be the group of geometric anthropomorphic figures.

Regarding the alteration crust, the superficial deposits are thicker in the lower part, on the left of the panel, and are thinner in the upper part, especially on the right side. The variable thickness of alteration deposits is linked to runoff deposits on the left part of the panel, clearly visible in Fig. 1. Interestingly, the DPK15-02 sample is located in the part of the panel displaying a higher rate of alteration crust formation whereas the pigment layer is the most superficial. Thus, we can propose that this figure is more recent than the rest of the panel. For the other figures, as the pigment layers are lying on the calcareous bedrock, it is impossible to determine the relative chronology of their appearance, except for the superficial painting layer DPK-04 that is obviously more recent.

Conclusion

The colored rocks and ochres from the archaeological site of DPK are homogeneous in terms of their mineralogical and elemental compositions which suggests a common geological origin. The source of procurement was probably local, due to the presence of As, an element present in large quantities in the geological formations of the Mae Mo Basin, a few kilometers from the site.

The presence of similar materials, both in the burial and in the surrounding archaeological levels, suggests a certain continuity in the exploitation of this geological source. On the other hand, the paintings on the walls have a greater variety of pigment compositions which indicates that the panels were created in different phases. The only painting pigment that corresponds to the materials identified in the archaeological levels and burials at DPK is that used for the anthropomorphic figures.

Without direct dating of elements, it is not possible to establish a direct link between the painting and burials. The presence of whewellite in the alteration crust overlaying the paintings could provide a 14C dating. The alteration crusts are mainly thin, but some areas displaying thicker deposits and overlaying figures could provide enough carbon for dating. Nevertheless, at this stage of our investigations, the discovery of two fragments of painted wall (I4-256 and I3-103) in the archaeological layer of DPK attest to a long tradition of rock painting for at least 11,000 years, which corresponds to one of the most ancient evidence of rock art in mainland Southeast Asia.

Acknowledgments

The fieldwork was undertaken under the authority of the 6th Archaeological Division of Fine Arts Department, Nan Museum, Thailand. We are grateful to Chaturaporn Tiamtinkrit and Chawalit Khaokhiew for their support. This work was supported by the French Ministry of Foreign Affairs and by the Muséum National d'Histoire Naturelle de Paris (MNHN) though ATM fundings. The authors also want to thank the Sorbonne Universités and the MH-SATSU-OPPaCro project for their financial participation and the preparation of samples by Manon Bondetti. We are grateful to the MNHN for access to its analytical platforms: the "DGD Collection" for the SEM analysis, the HNHP (UMR 7194) and the "Plateau de Caractérisation des Archéomatériaux et Archives Sédimentaires" for XRF analysis and sample preparation, and the "Plateau d'imagerie 2D/3D" for microscopy, and Marie-Madeleine Blanc-Valleron from the CRP2A (UMR 7207) for conventional XRD. We would also like to acknowledge the Sorbonne Université and especially the LAMS (UMR 8220) for μXRD and Monaris (UMR 8233) for Raman analysis. Finally, we would like to thank Becky Coles and anonymous reviewers for their constructive comments and improvements to this manuscript.

Bibliography

Bar-Yosef Mayer, D.E., Vandermeersch, B., Bar-Yosef, O., 2009. Shells and ochre in Middle Paleolithic Qafzeh Cave, Israel: indications for modern behavior, Journal of Human Evolution 56, 307-314.

Klima, B., 1987. A triple burial from the Upper Paleolithic of Dolní Věstonice, Czechoslovakia, Journal of Human Evolution 16, 831-835.

Thorne, A., Grün, R., Mortimer, G., Spooner, N.A., Simpson, J.J., McCulloch, M., Taylor, L., Curnoe, D., 1999. Australia's oldest human remains: age of the Lake Mungo 3 skeleton, Journal of Human Evolution 36, 591-612.

Henry-Gambier, D., 2002. Les fossiles de Cro-Magnon (Les Eyzies-de-Tayac,

Dordogne). Nouvelles données sur leur position chronologique et leur attribution

culturelle, Bull. et Mém. de la Société d'Anthropologie de Paris 14, 89-112.
O'Reilly, D.J.W., 2014. Increasing complexity and the political economy model; a consideration of Iron Age moated sites in Thailand, Journal of Anthropological Archaeology 35, 297-309.
Higham, C.F.W., 2011. The Iron Age of the Mun Valley, Thailand, The Antiquaries Journal 91, 101-144.
Imdirakphol, S., Zazzo, A., Auetrakulvit, P., Tiamtinkrit, C., Pierret, A., Forestier, H., Zeitoun, V., 2017. The perforated stones of the Doi Pha Kan burials (Northern Thailand): A Mesolithic singularity?, Comptes Rendus Palevol 16, 351-361.
Thong, P.T., 1980. Con Moong cave. A noteworthy archaeological discovery in Vietnam., Asian Perspectives 23, 17-21.
Ha, V.T., 1980. Nouvelles recherches préhistoriques et protohistoriques au Vietnam., Bulletin de l'Ecole Française d'Extrême-Orient 68.
Oxenham, M., 2006. Biological responses to change in prehistoric Vietnam., Asian Perspectives 45, 212-239.
Jacob, T., Soepriyo, A., 1994. A preliminary palaeoanthropological study of the Gua Gunung Runtuh hman skeleton., in: Zuraina, M. (Ed.), The excavation of Gua gunng Runtuh and the discovery of the Perak man in Malaysia, Department of Museums and Antiquities, Malaysia, Kuala Lumpur, pp. 48-69.
Zuraina, M., 1994. The excavation of Perak man, an epi-Palaeolithic burial at Gua Gunung Runtuh, in: Zuraina, M. (Ed.), The excavation of Gua gunng Runtuh and the discovery of the Perak man in Malaysia. Department of Museums and Antiquities, Malaysia, Kuala Lumpur, pp. 230–247.
Zuraina, M., Arif, J., Samsuddin, A.R., Nizam, A., Lim, A., Saidin, M., Abdujjah, J., Chia, S.,, 2005. GTK 1: a skeleton from Gua Teluk Kelawar, Lenggong dated 8,400±40 BP. , in: Zuraina, M. (Ed.), The Perak man and other prehistoric skeletons of Malaysia. , Penerbit Universiti Sains Malaysia, Pulau Pinang, pp. 345-361.
Van Heekeren, H.R., 1961. A preliminary note on the excavation of the Sai-Yok rock-shelter., Journal of the Siam Society 48, 99-108.
Jacob, T., 1969. The Mesolithic skeletal remains from Sai-Yok, in: Sangvichien, S., Sirigaroon, P., Jørgensen, J.B. (Eds.), Archaeological Excavations in Thailand, Vol. III: Ban-Kao. Part Two: The Prehistoric Thai Skeletons, Munksgaard, Copenhagen, pp. 49–52.
Doy Asa, T., Winayalai, C., Sangchan, W., 2001. A Search for the culture of three thousand years ago through the gate of Phratu Pha at Lampang, Department of Archaeology 6th office of FAD, Chiang Mai.
Srongsiri, W., Sangchan, W., 1997. Phratu Pha, Lampang, prehistorical site, "3,000 years" Rock painting Ceremony at the sacred cliff", Art and Culture Magazine, Sujit Wongtate, Bangkok., 135 p.
Tan, N.H., Taçon, P.S.C., 2014. Rock Art and the Sacred Landscapes of Mainland Southeast Asia, in: Gillette, D.L., Greer, M., Helene Hayward, M., Breen Murray, W. (Eds.), Rock Art and Sacred Landscapes, Springer New York, New York, NY, pp. 67-84.
Higham, C., 2002. Early Cultures of Mainland Southeast Asia, River Books, Bangkok.
Taçon, P.S.C., Tan, N.H., O'Connor, S., Xueping, J., Gang, L., Curnoe, D., Bulbeck, D., Hakim, B., Sumantri, I., Than, H., Sokrithy, I., Chia, S., Khun-Neay, K., Kong, S., 2014. The global implications of the early surviving rock art of greater Southeast Asia, Antiquity 88, 1050-1064.
Aubert, M., Brumm, A., Ramli, M., Sutikna, T., Saptomo, E.W., Hakim, B., Morwood, M.J., van den Bergh, G.D., Kinsley, L., Dosseto, A., 2014. Pleistocene cave art from Sulawesi, Indonesia, Nature 514, 223.
Aubert, M., O'Connor, S., McCulloch, M., Mortimer, G., Watchman, A., Richer-LaFlèche, M., 2007. Uranium-series dating rock art in East Timor, Journal of Archaeological Science 34, 991-996.

Aubert, M., Setiawan, P., Oktaviana, A.A., Brumm, A., Sulistyarto, P.H., Saptomo, E.W., Istiawan, B., Ma'rifat, T.A., Wahyuono, V.N., Atmoko, F.T., Zhao, J.X., Huntley, J., Taçon, P.S.C., Howard, D.L., Brand, H.E.A., 2018. Palaeolithic cave art in Borneo, Nature 564, 254-257.
Surinlert, J., Auetrakulvit, P., Zeitoun, V., Tiamtinkrit, C., Khemnak, P., 2018. Prehistoric Rock-Art at Doi Pha Kan, Lampang Province, Thailand, in: Tan, N. (Ed.), Advancing Southeast Asian Archaeology, , SEAMEO SPAFA Regional Centre for Archaeology and Fine Arts, Bangkok, pp. 380-382.
Jones, T., Levchenko, V.A., King, P.L., Troitzsch, U., Wesley, D., Williams, A.A., Nayingull, A., 2017. Radiocarbon age constraints for a Pleistocene–Holocene transition rock art style: The Northern Running Figures of the East Alligator River region, western Arnhem Land, Australia, Journal of Archaeological Science: Reports 11, 80-89.
Beck, L., Lebon, M., Pichon, L., Menu, M., Chiotti, L., Nespoulet, R., Paillet, P., 2011. PIXE characterisation of prehistoric pigments from Abri Pataud (Dordogne, France), X-Ray Spectrometry 40, 219-223.
Lebon, M., Beck, L., Gregoire, S., Chiotti, L., Nespoulet, R., Menu, M., Paillet, P., 2014. Prehistoric pigment characterization of the abri Pataud rock-shelter (Dordogne, France), **Open journal of Archaeometry. (PAGEPress Publications)** 2:5456, 90-94.
Chalmin, E., Hœrlé, S., Reiche , I., 2017a. Taphonomy on the Surface of the Rock Wall: Rock-Paint-Atmosphere Interactions, in: B., D., McNiven, I.J. (Eds.), The Oxford Handbook of the Archaeology and Anthropology of Rock Art, Oxford University Press, Online Publication, pp. 1-35.
Chalmin, É., Castets, G., Delannoy, J.-J., David, B., Barker, B., Lamb, L., Soufi, F., Pairis, S., Cersoy, S., Martinetto, P., Geneste, J.-M., Hoerlé, S., Richards, T., Gunn, R., 2017b. Geochemical analysis of the painted panels at the "Genyornis" rock art site, Arnhem Land, Australia, Quaternary International 430, 60-80.
Zeitoun, V., Auetrakulvit, P., Zazzo, A., Pierret, A., Frère, S., Forestier, H., 2019. Discovery of an outstanding Hoabinhian site from the Late Pleistocene at Doi Pha Kan (Lampang province, northern Thailand), Archaeological Research in Asia.
Surinlert, J., 2013. The study of Prehistoric rock-Art at Doi Pha Kan, Lampang province, Thailand., Master dissertation, Department of Archaeology, Silpakorn university, Bangkok.
Solé, V.A., Papillon, E., Cotte, M., Walter, P., Susini, J., 2007. A multiplatform code for the analysis of energy-dispersive X-ray fluorescence spectra, Spectrochim. Acta Part B 62, 63-68.
Casadio, F., Daher, C., Bellot-Gurlet, L., 2016. Raman Spectroscopy of cultural heritage Materials: Overview of Applications and New Frontiers in Instrumentation, Sampling Modalities, and Data Processing, Topics in Current Chemistry 374, 62.
Lafuente, B., Downs, R.T., Yang, H., Stone, N., 2015. The power of databases: the RRUFF project., in: Armbruster, T., Danisi, R.M. (Eds.), Highlights in Mineralogical Crystallography, W. De Gruyter, Berlin, Germany, pp. 1-30.
Dayet, L., Le Bourdonnec, F.X., Daniel, F., Porraz, G., Texier, P.J., 2016. Ochre Provenance and Procurement Strategies During The Middle Stone Age at Diepkloof Rock Shelter, South Africa, Archaeometry 58, 807-829.
Zipkin, A.M., Hanchar, J.M., Brooks, A.S., Grabowski, M.W., Thompson, J.C., Gomani-Chindebvu, E., 2015. Ochre fingerprints: Distinguishing among Malawian mineral pigment sources with Homogenized Ochre Chip LA–ICPMS, Archaeometry 57, 297-317.
Beck, L., Salomon, H., Lahlil, S., Lebon, M., Odin, G.P., Coquinot, Y., Pichon, L., 2012. Non-destructive provenance differentiation of prehistoric pigments by external PIXE, Nuclear Instruments and Methods in Physics Research Section B: Beam Interactions with Materials and Atoms 273, 173-177.
Mathis, F., Bodu, P., Dubreuil, O., Salomon, H., 2014. PIXE identification of the provenance of ferruginous rocks used by Neanderthals, Nuclear Instruments and Methods in Physics Research Section B: Beam Interactions with Materials and Atoms 331, 275-279.
Popelka-Filcoff, R.S., Miksa, E.J., Robertson, J.D., Glascock, M.D., Wallace, H., 2008. Elemental analysis and characterization of ochre sources from Southern Arizona, Journal of Archaeological Science 35, 752-762.

Morley, C.K., Racey, A., 2011. Tertiary stratigraphy, in: Ridd, M.F., Barber, A.J., Crow, M.J. (Eds.), The Geology of Thailand, Geological Society of London, pp. 223-271

Jitapankul, S., Charussuriyong, P., Jantanachotivot, S., 1985. Geology of Tertiary deposit of Mae Moh basin, Proc. Confer. Lignite Indust. in Thailand, Elec. Generating Auth. of Thailand, Thailand,, 1-16.
Ratanasthien, B., Takashima, I., Matsubaya, O., 2008. Paleaogeography and Climatic Change recorded on Viviparidae Carbon and Oxygen Isotope in Mae Moh Coal Mine, Northern Thailand, Bulletin of the Geological Survey of Japan 59, 327-338.
Vichaidid, T., Limsuwan, S., Limsuwan, P., 2012. American Journal of Applied Sciences American Journal of Applied Sciences 9, 1329-1336.
Bashkin, V.N., Wongyai, K., 2002. Environmental fluxes of arsenic from lignite mining and power generation in northern Thailand, Environmental Geology 41, 883-888.
Mamindy-Pajany, Y., Hurel, C., Marmier, N., Roméo, M., 2009. Arsenic adsorption onto hematite and goethite, Comptes Rendus Chimie 12, 876-881.
Giménez, J., Martínez, M., de Pablo, J., Rovira, M., Duro, L., 2007. Arsenic sorption onto natural hematite, magnetite, and goethite, Journal of Hazardous Materials 141, 575-580.
Palache, C., Berman, H., Frondel, C., 1951. The system of mineralogy, volume II.
Vieillefon J., 1973. Compte rendu du symposium sur les sols acides à sulfates (Wageningen, Pays-Bas, août 1972). Cahiers ORSTOM série Pédologie 11, 193-198.
Marius C., 1981. Caractéristiques et utilisations de quelques sols sulfaté-acides de Thaïlande et Malaisie, ORSTOM Paris / Université Louis Pasteur, Institut de Géologie Strasbourg, 22 p.
Bell, I.M., Clark, R.J.H., Gibbs, P.J., 1997. Raman spectroscopic library of natural and synthetic pigments (pre- ≈ 1850 AD), Spectrochimica Acta Part A: Molecular and Biomolecular Spectroscopy 53, 2159-2179.
Frost, R.L., 2004. Raman spectroscopy of natural oxalates, Analytica Chimica Acta 517, 207-214.
Middleton, A.P., Edwards, H.G.M., Middleton, P.S., Ambers, J., 2005. Identification of anatase in archaeological materials by Raman spectroscopy: implications and interpretation, Journal of Raman Spectroscopy 36, 984-987.
Pagès-Camagna, S., Duval, A., Guicharnaud, H., 2004. Study of Gustave Moreau's black drawings: identification of the graphic materials by Raman microspectrometry and PIXE, Journal of Raman Spectroscopy 35, 628-632.
Scott, D.A., Hyder, W.D., 1993. A study of some californian indian rock art pigments, Studies in Conservation 38, 155-173.
Watchman, A., Ward, I., Jones, R., O'Connor, S., 2001. Spatial and compositional variations within finely laminated mineral crusts at Carpenter's Gap, an archaeological site in tropical Australia, Geoarchaeology 16, 803-824.
Russ, J., Kaluarachchi, W.D., Drummond, L., Edwards, H.G.M., 1999. The nature of a whewellite-rich rock crust associated with pictographs in southwestern Texas, Studies in Conservation 44, 91-103.
Roberts, A., Campbell, I., Pring, A., Bell, G., Watchman, A., Popelka-Filcoff, R., Lenehan, C., Gibson, C., Franklin, N., 2015. A multidisciplinary investigation of a rock coating at Ngaut Ngaut (Devon Downs), South Australia, Australian Archaeology 80, 32-39.
Ford, B., MacLeod, I., Haydock, P., 1994. Rock art pigments from Kimberley region of Western Australia: identification of the minerals and conversion mechanisms, Studies in Conservation 39, 57-69.
Del Monte, M., Sabbioni, C., Zappia, G., 1987. The origin of calcium oxalates on historical buildings, monuments and natural outcrops, Science of The Total Environment 67, 17-39.
Del Monte, M., Sabbioni, C., 1984. Gypsum crusts and fly ash particles on carbonatic outcrops, Archives for meteorology, geophysics, and bioclimatology, Series B 35, 105-111.
Siedel, H., Pfefferkorn, S., von Plehwe-Leisen, E., Leisen, H., 2010. Sandstone weathering in tropical climate: Results of low-destructive investigations at the temple of Angkor Wat, Cambodia, Engineering Geology 115, 182-192.

Gömez-Heras, M., Benavente, D., Alvarez de Buergo, M., Fort, R., 2004. Soluble salt minerals from pigeon droppings as potential contributors to the decay of stone based Cultural Heritage, European Journal of Mineralogy 16, 505-509.
Watchman, A., 1990. A review of studies into the composition of pigments used in Australian rock paintings Journée internationales d'étude sur la conservation de l'art rupestre "50 ans aprés la découverte de Lascaux" Dordogne - Perigord (France), 20–23 aout 1990, Proceedings of the ICOM Conference. Edit. Atelier de Recherches et d'Etudes en Perigord, 21-28.

Sample ID	Sample description	Archaeological Unit / Grave
Raw pigments		
DPK-2013-D3-T1	Raw pigment	Archaeologicallayer
DPK-2011-E4-280	Raw pigment	Archaeologicallayer
DPK-2011-E4-282	Raw pigment	Archaeologicallayer
DPK-2011-E4-283	Raw pigment	Archaeologicallayer
DPK-2011-E4-286	Raw pigment (powdered)	Archaeologicallayer
DPK-2011-E5-317	Raw pigment (faceted)	Grave E5
DPK-E5-B1	Raw pigment (powdered)	Grave E5
DPK-2013-F3-437	Raw pigment	Archaeologicallayer
DPK-2014-G5-310	Raw pigment	Archaeologicallayer
DPK-2014-G6-32	Raw pigment	Archaeologicallayer
Colouredartefacts and artifacts covered by pigments		
DPK-2012-D6-323	Grinding stone with pigment	Archaeologicallayer
DPK-2015-I3-103	Fragment of pebble with pigment	Archaeologicallayer
DPK-2012-D7-413	Decoratedpebble	Archaeologicallayer
DPK-2011-E5-15	Couloured artefact	Archaeologicallayer
DPK-2011-E5-288	Couloured pendant	Grave E5
DPK-2014-G6-119	Perforated stone	Archaeologicallayer
Fragments of wall with pigments		
DPK-2015-I3-425	paintedcalcarousflake	Archaeologicallayer
DPK-2015-I4-256	paintedcalcarousflake	Archaeologicallayer
Samples of painting from wall		
DPK-2015-01	Unidentified - Pigment on altered area	Painted wall
DPK-2015-02	Group III - Elephant	Painted wall
DPK-2015-03	Group II - Geometricform	Painted wall
DPK-2015-04	Group II - Bovid	Painted wall
DPK-2015-05	Group I - Anthropomorphs	Painted wall
DPK-2015-06	Group I - Geometricform	Painted wall

Table 1 : List, description and origin of analyzed samples

	Al (wt%)	Si (wt%)	Cl (wt%)	Ca (wt%)	Fe (wt%)	As (wt%)
DR-N (Diorite)						
XRF Measurement	11,3	24,2	0,14	5,6	7,0	0,00
Reference Value	*9,3*	*24,7*	*0,04*	*5,0*	*6,8*	*0,00*
BX-N (Bauxite)						
XRF Measurement	24,9	5,8	0,26	0,3	16,9	0,01
Reference Value	*28,7*	*3,5*	*0,00*	*0,1*	*16,2*	*0,01*
CHR-Pt+ (Chromitite)						
XRF Measurement	7,0	12,9	0,04	0,2	8,1	0,04
Reference Value	*3,9*	*10,2*	*0,00*	*0,2*	*9,4*	*0,04*
UB-N (Serpentine)						
XRF Measurement	4,3	18,5	0,12	0,8	5,7	0,00
Reference Value	*1,5*	*18,4*	*0,08*	*0,9*	*5,8*	*0,00*

Table 2: Concentration of main elements detected in DPK archaeological samples (Al, Si, Cl, Ca, Fe, and As) measured by XRF for four SARM geostandards (DR-N ; BX-N ; CHR-Pt+ ; UB-N) and compared with references values

Sample ID	**Sample description**	**XRD**	**µXRD**	**XRF**	
Raw pigments and colored artifacts				**Major,** Minor, *Traces*	**Specific element**
DPK-2013-D3-T1	Raw pigment		**Hematite**	**Fe, Al, Si**,*K*	As
DPK-2011-E4-280	Raw pigment		**Hematite**, Quartz, *Kaolinite?*	**Fe, Al, Si**,*K*	As
DPK-2011-E4-282	Raw pigment		**Hematite**, *Quartz, Kaolinite ?*	**Fe, Al, Si**,*K*	As
DPK-2011-E4-283	Raw pigment		**Hematite**, Quartz	**Fe, Al, Si**,*K*	As
DPK-2011-E4-286	Raw pigment (powdered)	**Hematite, Quartz, Calcite,** Kaolinite		**Fe, Si,** Al, Ca, *K, Mn, As*	As, Mn
DPK-2011-E5-317	Raw pigment (faceted)		**Quartz,** *Hematite*	**Fe, Si**,Al, *K*	As
DPK-E5-B1	Raw pigment (powdered)	**Hematite, Quartz,** Goethite, Kaolinite		**Fe,** *Al, Si, K, Ca, As*	As
DPK-2013-F3-437	Raw pigment		**Hematite**	**Fe, Al, Si,** K, Ca	As
DPK-2014-G5-310	Raw pigment		Un-identified	**Fe,** *Al, Si, Ca, As*	As
DPK-2014-G6-32	Raw pigment	**Hematite, Quartz,** Goethite, Kaolinite, Alunite, Jarosite	**Hematite,** Goethite, Halite ?	**Fe, K,** Al, Si, Ca, S, *Cl*	S, Cl
DPK-2011-E5-15	Couloured artefact		**Quartz**, *Goethite ?*	**Si, Al**, Fe, *Ca, K, S*	
DPK-2011-E5-288	Couloured pendant		**Calcite, Quartz,** *Goethite, Hematite ?*	**Si,** Al, Fe,*K, Ca*	
Artifacts covered by pigments					
DPK-2012-D6-323	Grinding stone with pigment		**Hematite, Quartz**	**SI, Fe,** Al, Ca	As
DPK-2015-I3-103	Fragment of pebble with pigment		Un-identified	**Ca, Si,** Al, Fe	As
DPK-2012-D7-413	Painted calcareous pebble		**Calcite, Dolomite,** *Hematite*	**Ca, Si,** Al, Fe	As
DPK-2014-G6-119	Perforated stone		**Calcite, Dolomite,** *Hematite*	Not accessible	Not accessible

Table 3: Summery of mains results obtained by X-Ray diffraction (XRD), micro-X-Ray diffraction (µXRD) and X-Ray fluorescence spectrometry (XRF)

	Alteration crusts			Painting layers				
	Thinkness	Main mineral phases	Othermineral phases detected	Thickness	Relative position	Composition	Size of iron oxide grains	Comments
DPK15-01	100-150 µm	Gypse, Calcium oxalate (Whewellite)	Calcium phosphate, Calcite	-	-	-		-
DPK15-02	40-80 µm	Gypse, Calcium oxalate (Whewellite)	Calcium phosphate, barium sulfate, strontium sulfate	20-30 µm	Superficial part of the alteration layer	IronOxides, Aluminosilicates, few Quatz grains	1 - 10 µm	Fribrousclays
DPK15-03	50 - 80 µm	Gypse, Calcium oxalate (Whewellite)	TitaniumOxide, Calcium phosphate	20 µm	Deeper part of the alteration layer	IronOxides, Aluminosilicates, and Quartz grains	1 - 15 µm	Large grains of clays
DPK15-04	50 à 100 µm	Gypse, Calcium oxalate (Whewellite)		> 10-20 µm	In the middle of the alteration crust	IronOxides, Aluminosilicates	≈5 µm	
				<10 µm	Deeper part of the alteration layer	IronOxides, Aluminosilicates, and Quartz grains	≈5 µm	
DPK15-05	20-50 µm	Gypse, Calcium oxalate (Whewellite)	TitaniumOxide, Calcium phosphate	5-10 µm	Deeper part of the alteration layer	IronOxides, few Aluminosilicates	< 3-4µm	Presence of As
DPK15-06	10-50 µm	Gypse, Calcium oxalate (Whewellite)	Calcium phosphate	10-100 µm	Deeper part of the alteration layer	IronOxides, Aluminosilicates	mostly < 1 µm (few larger ones≈ 20 µm)	Fibrous clays, presence of As

Table 4: Description of alteration crusts and pigments layer from the DPK painted wall